2010-01-01

Hybrid Manufacturing: Integrating Stereolithography and Direct Print Technologies

Amit Lopes
University of Texas at El Paso, ajlopes@utep.edu

HYBRID MANUFACTURING: INTEGRATING STEREOLITHOGRAPHY AND DIRECT PRINT TECHNOLOGIES

AMIT JOE LOPES

Materials Science and Engineering

APPROVED:

_____
Ryan B. Wicker, Ph.D., Chair

_____
Eric MacDonald, Ph.D.

_____
Lawrence E. Murr, Ph.D.

_____
Felicia S. Manciu, Ph.D.

_____
Carl W. Dirk, Ph.D.

_____
Patricia D. Witherspoon, Ph.D.
Dean of the Graduate School

This dissertation is dedicated to my beloved family for their love and support. They are my source of inspiration, perseverance, hard work, humility, and happiness.

'What you do in life, echoes in eternity' ----- Gladiator

HYBRID MANUFACTURING: INTEGRATING STEREOLITHOGRAPHY AND DIRECT PRINT TECHNOLOGIES

by

AMIT JOE LOPES, M.S.

DISSERTATION

Presented to the Faculty of the Multidisciplinary Program

in Materials Science and Engineering of

The University of Texas at El Paso

in Partial Fulfillment

of the Requirements

for the Degree of

DOCTOR OF PHILOSOPHY

Materials Science and Engineering

THE UNIVERSITY OF TEXAS AT EL PASO

December 2010

ACKNOWLEDGMENTS

I would like to sincerely thank my advisor, Dr. Ryan B. Wicker, for allowing me to be part of his wonderful research group and perform the projects presented in this dissertation. I appreciate his guidance, knowledge, assistance, patience and all his support that helped me throughout my graduate studies. I enjoyed our numerous discussions about life in general which enabled me to become a responsible, mature individual. I would also like to thank my other committee members Dr. Eric MacDonald, Dr. Larry Murr, Dr. Felicia Manciu, and Dr. Carl Dirk for their guidance and knowledge throughout this project.

I would like to acknowledge my financial support for this research provided by the University of Texas at El Paso Graduate School (including the Dodson Dissertation Fellowship), and by scholarship from the UTEP Track and Field. I specially thank Mr. Robert Kitchens, former Head Coach at UTEP Track and Field, for all his help and advice on how to achieve excellence in everything I do. I would like to thank Dr. Ricardo Pineda for his support during the final stages of my dissertation.

I would like to thank all the Keck Center group members, both past and present, for their assistance during the course of this research. Special thanks to Frank Medina, Mahesh Tonde, Dr. Karina Arcaute, and Asim Inamdar for their helpful support at the beginning of this project. I would like to express my sincere gratitude to the student assistants and office secretaries including Liz Pardo, KiraLise Silva, and Alex Cooper for their assistance in numerous ways. I would like to acknowledge Dan Muse, Mohammed Alawneh, Richard Olivas, Rudolfo Salas, and Eric De Nava for their willingness to work extra hard with me to make this research happen, and to all the students that helped me on this research. I express sincere thanks to David Roberson

for his help on the use of the SEM for this research. Special thanks to Dr. In Hwan Lee for helping me finish the final experiments required for completing this dissertation.

I sincerely thank Mahesh Tonde, Bhupendra Kenjale, Ameet Chavan, and Bixler Paul for their friendship and companionship throughout my time here at UTEP. I truly appreciated the enjoyable conversations, adventure road trips and sports tours, amazing get-togethers, and all the great times spent together.

My deepest and most sincere gratitude goes to my beloved family including my parents: Joseph Alex Lopes and Mary Joseph Lopes, my adoring bother Sumit and sister-in-law Nisha, my loving wife Swapnali and my wonderful son Asher, for all their support and sacrifices. Thanks for being the pillars that I could lean on through the good and bad times, for always being there for me, and for being my source of inspiration, perseverance, hard work, humility, and happiness.

This thesis was submitted to the supervising committee in October, 2010.

EXECUTIVE SUMMARY

The focus of this research was the development of a hybrid manufacturing system that integrates stereolithography (SL) and direct print (DP) technologies to fabricate three dimensional (3D) structural electronic devices within a single set-up. The capabilities of this new additive manufacturing (AM) technology was explored in the context of fabricating and prototyping complex electronic devices in which conformal shape, rugged and light-weight integration, and a natural resistance to reverse engineering are all of paramount importance. Consequently, electronic components can be tightly integrated together in a rugged, light-weight 3D structure of arbitrary form. This research is a continuing advancement of the Mesoscopic Integrated Conformal Electronics (MICE) program which was developed at the Defense Advanced Research Projects Agency (DARPA) with a primary goal to develop direct write (DW) electronics applications for advancing the traditional IC manufacturing. It was during the developments as part of the MICE program that the concepts for integration of AM and DP for producing functional, monolithic 3D structures with embedded electronics emerged. Several researchers have since explored a variety of AM and DP systems, including multi-material technologies for fabricating unique functional products including structural electronic devices. Early developments in this research included the fabrication of multilayer circuitry and a manufacturing process for fabricating 2D electronic devices using separate SL and DP systems. Due to significant improvements in both the SL/DP process in recent years an increased level of sophistication of the integrated electronics has been achieved. These developments have culminated into the current work that describes a fully integrated system and a corresponding process that enables fabrication of complex, 3D structural electronic devices within a single integrated manufacturing environment.

As a result, this dissertation broadly demonstrated what can be achieved by integrating multiple AM technologies together for fabricating unique devices. Specifically, a hybrid SL/DP machine that can produce 3D monolithic structures with embedded electronics and printed interconnects is demonstrated. Advancements in the development of a hybrid manufacturing system that integrates SL and DP technologies to fabricate 3D structural electronic circuits are described. These advancement lead to the development of the state-of-the-art hybrid SL/DP system which included a 3D Systems SL 250/50 machine and an nScrypt micro-dispensing pump integrated within the SL machine through orthogonally-aligned linear translation stages for accurate 3D material dispensing. The 3D micro-dispensing DP system provided control over conductive trace deposition and combined with the manufacturing flexibility of the SL machine enabled the fabrication of monolithic 3D electronic structures. A corresponding manufacturing process was also developed using this system to fabricate 3D monolithic structures with embedded electronic circuits without removal from the hybrid SL/DP machine during the process. The process required multiple starts and stops of the SL process, removal of uncured resin from the SL substrate, insertion of active and passive electronic components, DP, *in situ* UV laser curing of the conductive traces.

As a key enabler of 3D structural electronic device fabrication, *in situ* UV laser ink curing of particulate silver based conductive inks was investigated further. Various laser curing parameters, including laser power, scan speed and time of laser incidence, laser scanning location, and laser wavelength were investigated through a series of experiments. The trace resistances for each experiment were compared to determine the laser conditions that resulted in the most effective ink curing. As part of this research, the laser energy supplied by the 355nm SL laser was related to an effective steady-state curing temperature as determined by a

commercially available thermistor. Scanning the laser on the edge of the ink channel gave the best ink curing, measured in terms of lowest trace resistance, but resulted in charring of the SL substrate. Alternatively, the laser condition at which the substrate did not char provided relatively less effective ink curing. Scanning the laser directly on the ink resulted in some discoloration, although SEM images revealed no structural changes. The effect of laser wavelength on trace resistance during repetitive laser curing was determined. Laser curing at 325 nm wavelength was found to be more effective than at 355 nm wavelength due to reduced reflectance of the silver particles at 325 nm wavelength. This research determined the experimental conditions for successful *in situ* UV laser curing of particulate silver-based inks in the context of fabricating 3D structural electronic devices using a hybrid SL/DP machine and advanced the capabilities of AM technologies. Opportunities exist for expanding the laser parameters to generalize the laser curing process for a variety of conductive inks. The electronic devices demonstrated as part of this research were simple 555 timer circuits designed and fabricated in 2D (single layer of routing) and 3D (multiple layers of routing and component placement).

In summary, a new methodology is presented for manufacturing non-traditional electronic systems in arbitrary form, while achieving miniaturization and enabling rugged structure and advanced applications are demonstrated using a semi-automated approach to SL/DP integration. Although the process does not require removal of the structure from the machine during fabrication, many of the current sub-processes are manual. As a result, further research should focus on the automation and development of many of the sub-processes to optimize the overall manufacturing process.

TABLE OF CONTENTS

LIST OF TABLES

LIST OF FIGURES

Chapter 1

1 INTRODUCTION

The goal of this research was the development of a hybrid manufacturing system that integrated stereolithography (SL) and direct print (DP) technologies in order to fabricate three dimensional (3D) structural electronic devices. The following sections give a brief introduction to the 3D structural electronics fabrication concept and describe the various developments that advanced the research. Section one explains the background and previous research that led to the development of alternate methods for fabricating integrated circuit (IC). Section two outlines the specific objectives for this research. Section three describes the development of the hybrid SL/DP system and corresponding process for fabricating simple 2D (single layer of routing) and 3D (multiple layers of routing and component placement) 555 timer circuits. Section four investigates *in situ* UV laser curing of the conductive ink traces and helps determine the most effective laser curing conditions. Using this technology, were designed and fabricated. The final section outlines the conclusions from this research and future areas of research that are essential to optimize the SL/DP technology.

1.1 Background on 3D Structural Electronics:

The development of Integrated Circuits (IC) and fabrication of structural electronic devices continually present new opportunities for manufacturing innovation. Traditionally, IC consists of Printed Circuit Board (PCB), which interconnects electronic components using flat conductive traces laminated onto a non-conductive substrate. However, the chemical processes required during PCB manufacturing processes leads to waste of materials and are not environmentally friendly. Furthermore, the electronic components on a PCB have reduced placement freedom and increased space requirements as they are generally placed in a planar

array on the board. As a result, by embedding electronic components within truly 3D dielectric substrates at various depths, a substantial reduction in circuit volume and weight can be realized as compared to traditional PCB. For advancing this concept, the Mesoscopic Integrated Conformal Electronics (MICE) program was developed at the Defense Advanced Research Projects Agency (DARPA), with a primary goal to develop Direct Write (DW) electronics fabrication tools onto conformal surfaces, without masks, and at low temperature. The MICE program led to the development and fabrication of electronics, sensors, and antennas on conformal surfaces as an alternative for tradition IC manufacturing using PCB to enhance the robustness of electronic systems while achieving significant weight savings for military applications. Through this program, manufacturing tools that directly write electronic components such as resistors, capacitors, and antennas, on a variety of substrates were developed. This significantly decreased processing complexity and cost with faster fabrication times. During these developments the concepts for integrating additive manufacturing (AM) and DP for producing functional, monolithic 3D structures with embedded electronics emerged.

As part of these developments, several researchers have explored a variety of AM and DP systems, including multi-material systems for fabricating unique functional products, including structural electronic devices (Lopes et *al.*, 2010). Specifically, Weiss and Prinz (1998) manufactured a novel waterproof wearable computer with embedded electronics using a shape deposition manufacturing technology. Church *et al.* (2000) demonstrate the capabilities of an advanced DP system to created wireless sensor systems. Pique *et al.* (2006) fabricated two dimensional (2D) embedded electronic circuits using flexible substrates by utilizing a laser direct write process. Robinson *et al.* (2006) demonstrated the capabilities of the Ultrasonic Consolidation (UC) technology integrated with DP ink dispensing to fabricate electronic

circuitry, antennae and other devices directly into a solid metal structure. Malone and Lipson (2006) developed novel material formulations to fabricate ionomeric polymer-metal composite actuators using the Fab@Home AM machine. As an advancement of this research, stereolithography (SL) was investigated as a potential AM technology that can be integrated with DP system to fabricate 3D structural electronic systems. Kataria and Rosen (2001) utilized the in-process start and stop feature of the SL machine to embed functional inserts within the SL substrate during the build. This research demonstrated that embedding virtually any component including electronics within an SL matrix is possible. Exploring this potential further, lead to the preliminary research that eventually resulted in the development of the hybrid SL/DP system and selection of the machines and materials needed to facilitate the integration of the two technologies.

SL is a three-dimensional printing layer-additive process to enable rapid generation of physical objects directly from a CAD (computer aided design) database (Jacobs, 2002). SL provides relatively better accuracy and surface finish than other RP technologies available today. The unique layer-by-layer building process of SL technology helps manufacture complex 3D parts. The ability to start and stop the build at any given layer enables the embedding of electronic components for manufacturing conformal embedded 3D electronic systems. SL presents distinct advantages that facilitate integration with other technologies including easy access to the build chamber, flexible optics, high accuracy of parts, and a variety of build materials (Figure 1.1a). DW and DP refer to any technique capable of transferring and/or processing a variety of materials over different substrates in a preset pattern (Chrisey and Pique, 2002).

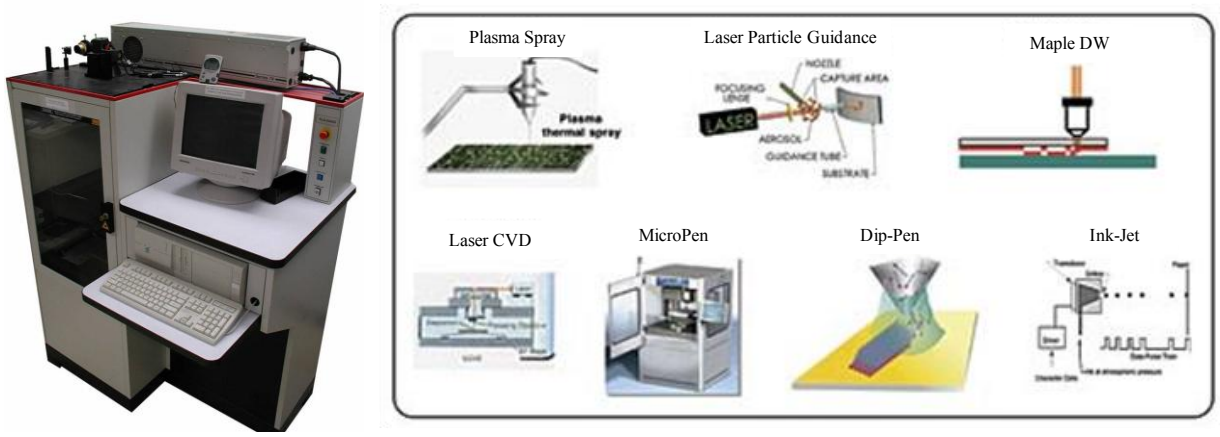

(a) (b)

Figure 1.1. (a) The SL system, (b) DW/DP techniques (Young *et al.*, 2005)

DW/DP manufacturing complements the field of AM and can be used for fabricating passive 3D structures and functional prototypes (Young et al., 2005). With this background, the objective of this research was to develop an integrated SL/DP system to enable the fabrication of monolithic 3D electronics structures in arbitrary form for unique applications.

1.2 Preliminary Research:

This section describes the preliminary research conducted by our group for integrating SL and DP technologies. Early developments in this research included the fabrication of functional electronic devices using separate SL and DP systems (Palmer *et al.*, 2004). Additionally, successful *in situ* laser conductive ink curing process was demonstrated by utilizing the flexibility of the SL system to incorporate vias, and strategic build start and stop along with control over the laser power (Medina *et. al.*, 2005). A second generation hybrid SL/DP machine was utilized for fabricating a simple 2D 555 timer circuit (Lopes *et al.*, 2006). These preliminary experiments provided proof of concept for pursuing this research.

1.2.1 Demonstration of Multilayer Circuitry Using the First Generation Hybrid SL/DP System

This research presents the first efforts at combining the advantages of RP technology with DP ink dispensing technology in an integrated manufacturing environment with a goal to fabricate functional embedded electronic systems. As a result, a combined SL and DP system was utilized to fabricate a sample SL part with embedded electrical circuitry and vertical interconnection between the multiple DP routing layers (Medina *et al.*, 2005). Figure 1.2 illustrates the first generation hybrid SL/DP system that was utilized to fabricate a SL part with two separate DP layers and a vertical interconnection between the two (providing 3D circuitry). Figure 1.2 illustrates the necessary components for successful integration of SL and DP technologies and additional details of the operation are provided in the Medina *et al.* (2005).

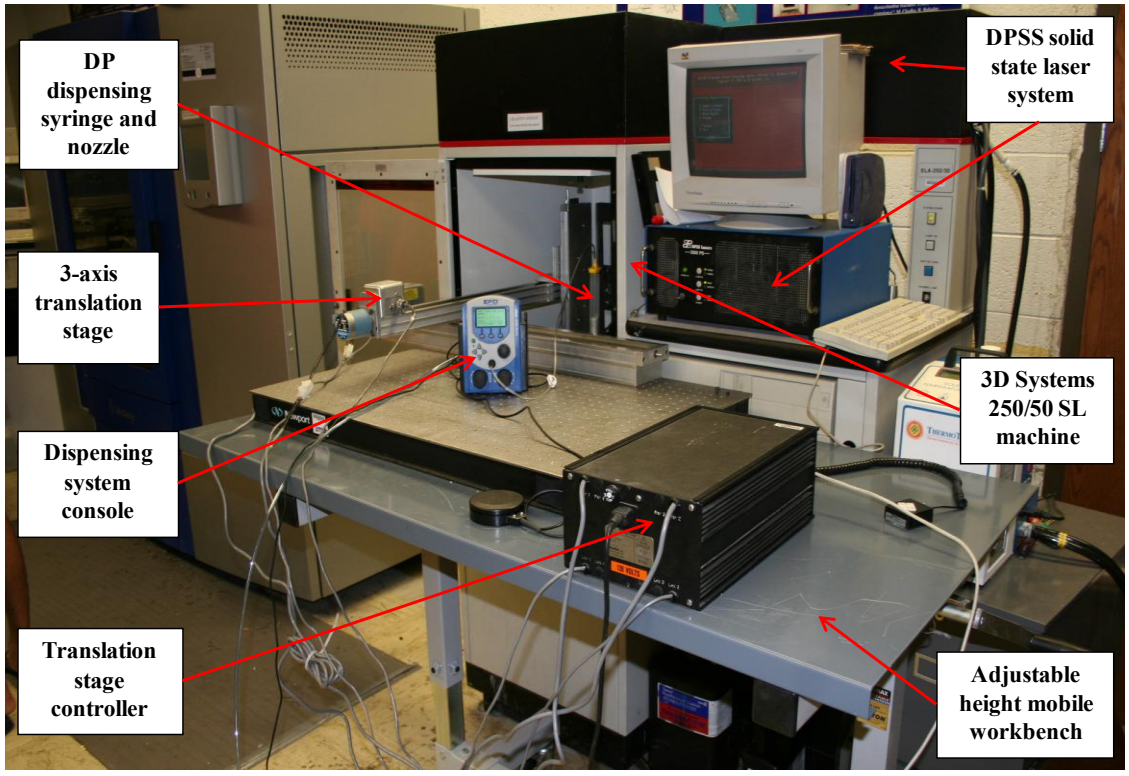

Figure 1.2. The first generation hybrid SL/DP system

The first generation hybrid SL/DP setup, described in Medina *et al.* (2005) was used to manufacture a simple part with embedded circuitry. A standard SL 250/50 systems ((3D Systems Inc., Rock Hill, SC) was combined with a three axis orthogonally aligned linear stages (Velmex Inc., Bloomfield, NY) to develop the hybrid SL/DP system. The DP setup was placed on a custom-made hand-crank height adjustable table two legged mobile workbench (Part # 9054T113 and Part # 3517T82, respectively, McMaster-Carr Supply Company, Chicago, IL). The Ultra 2405 dispensing system (EFD® Inc., East Providence, Rhode Island) syringe was attached to the z-stage of the orthogonally aligned three-axis traverse system. The CI 1002 conductive ink (ECM, Delaware, OH) utilized as ink material for the conductive traces required a high temperature to cure (110 ˚C for 15 minutes). As a result, DSM Somos® ProtoTherm™ 12120 (DSM Somos®, Elgin, IL) resin was selected as the substrate material due to its ability to withstand high temperatures (HDT up to 126 ˚C). SolidWorks® CAD modeling software was used to generate the part design, which was further converted into the required STL format using 3D Systems proprietary slicing software, 3D Lightyear™ 1.4.

Figure 1.3 illustrates the various steps for fabricating an SL part with interconnected multi-layer circuitry. The SL/DP process was initiated by building the SL base with a strategically placed in-built 0.025" diameter cylindrical via having 0.008" depth, which was utilized as the starting point for the DP process (‗Build SL base' in Figure 1.3). Once a predetermined build layer was reached, the vat was lowered to expose the top surface. The surface was cleaned using iso-propyl-alcohol prior to the DP process. Any remaining uncured resin was cured by scanning the top layer with the SL laser to ensure no contamination between the resin and the ink. The Ultra 2405 dispensing system syringe was attached to the orthogonally aligned three-axis traverse was then registered with the SL part starting point described

preciously and utilized to dispense the conductive ink in the required pattern (‗Register SL/DP' in Figure 1.3). The DP system was then controlled using LabVIEW® to replicate the required DP profile and dispense the ink to complete the ink trace (‗DP' in Figure 1.3).

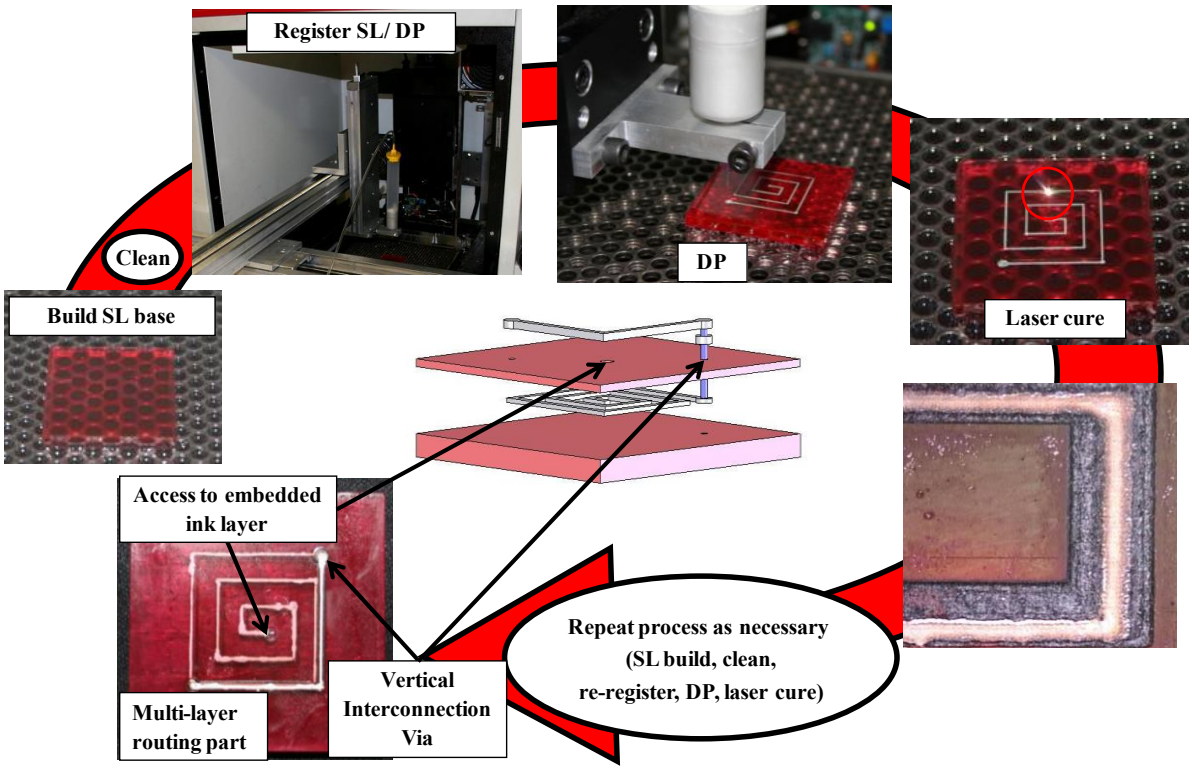

Figure 1.3. Fabrication process steps for realizing multilayer circuitry

After completion of the DP process at this layer, the ink was cured using the diode-pumped solid-state (DPSS) SL laser (Series 3500-SMPS, DPSS Lasers Inc., Santa Clara, CA). The laser power was manually adjusted to 100 mW during the ink curing process, and the depth of penetration of the resin was also reduced from 6-mils to 1.25-mil in order to obtain increased localized heating for ink curing at low scanning speeds (<0.020 in/sec). The laser was commanded to follow the deposited ink using a ‗.stl' file that matched the dispensed trace (‗Laser cure' in Figure 1.3). The effect of curing was investigated by testing the resistivity using a MeTex® multimeter (Model # M–3850D, MeTex® Corp., Seoul, Korea). The laser curing process (10 laser passes at 3 minutes and 40 seconds per trace or 37 total minutes and 100 mW

laser power) resulted in a volumetric resistivity value of ~127 μΩ-cm which was close to the resistivity value recommended by the ink manufacturer (~89 μΩ-cm). After completing the ink curing process, the SL vat was re-leveled and the SL build was continued to encapsulate the laser cured DP ink trace. The build was again interrupted at the SL layer where the second DP layer was required to be deposited. After repeating the cleaning process described earlier, the second DP interconnect was deposited on the SL substrate and the laser curing process was repeated. To provide vertical interconnection, a via connecting the two DP routing layers was incrementally filled with conductive ink and cured using the same SL laser curing conditions. The finished part, as shown in Figure 1.3, features a vertical interconnect via and a access via that was utilized to test 3D conductivity

This work demonstrated the use of a 355 nm DPSS laser for satisfactorily curing a conductive ink trace which was dispensed during the hybrid manufacturing process. The *in situ* laser ink curing process allowed the SL build to continue without removing the part from the platform and enabled multilayer circuitry. This feature can potentially enable embedding electronic components in 3D while providing electrical connections at various stages during the build. However, excess charring of the substrate and larger cure widths required to compensate for registration inaccuracies were areas of future research and provided motivation for some of the research in this dissertation.

1.2.2 Fabrication of a simple 2D 555 Timer Circuit Using a Second Generation Hybrid SL/DP System

Lopes *et al.* (2006) presented a second generation hybrid SL/DP system that was utilized for manufacturing embedded electronic components in a semi-automated environment with DP interconnects. In this research the 3-axis traverse system was upgraded from the previous

research for providing enhanced automation and control over the stages. The upgraded SL/DP system was utilized to embed electronic components within a SL part and the interconnects between the components were completed using DP. Figure 1.4 illustrates the second generation hybrid SL/DP manufacturing system that combines a SL 250/50 machine and the Ultra 2405 dispensing system, described in the previous system.

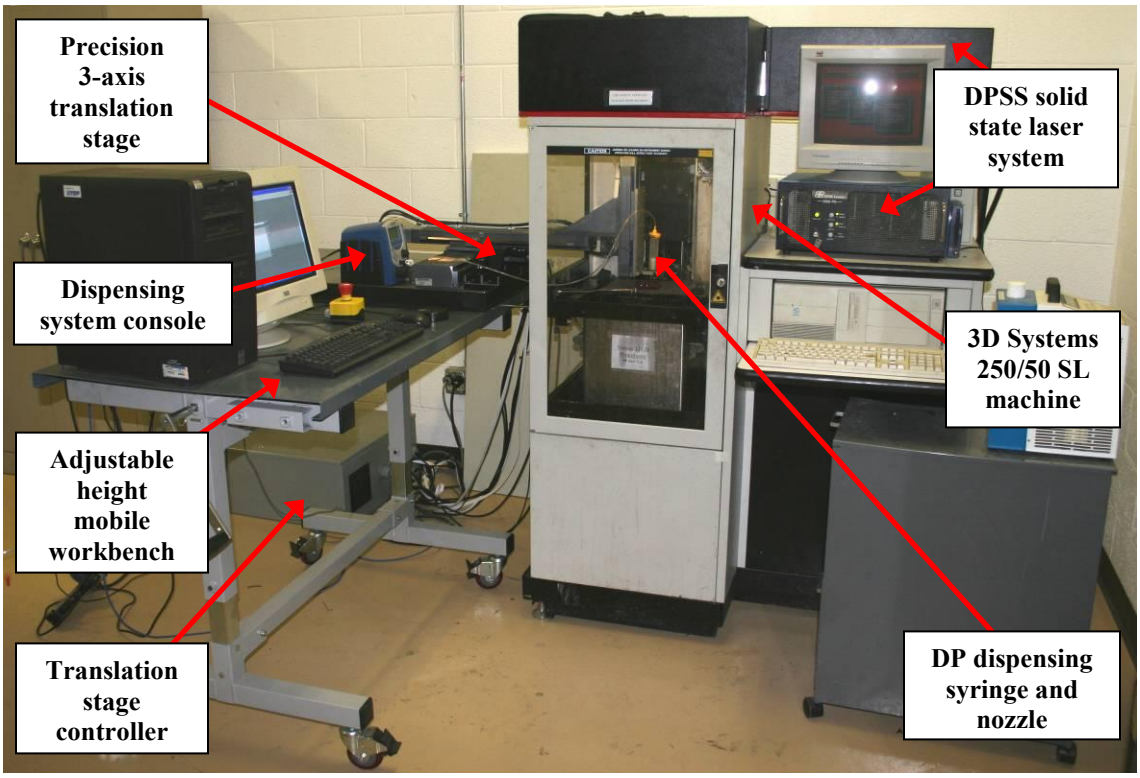

Figure 1.4. The second generation hybrid SL/DP system (Lopes *et al.*, 2006)

The DP setup was placed on a stainless steel top, adjustable-height hand-crank two legged custom-made mobile workbench. The 3-axis movement was achieved by orthogonally aligned upgraded precision linear positioning stages with direct drive precision ground screw drives and built-in 0.1 µm resolution linear encoders (LM150D-0400 model and LM100D-0100 model, Parker Hannifin Corporation, Electromechanical Automation Division, Rohnert Park, California). The Ultra 2405 dispensing system, combined with the advanced 3-axis traverse

stages, enabled precise dispensing of the conductive ink traces. As described earlier, ProtoTherm™ 12120 was selected as the resin for this research due to its high heat tolerance and relatively low viscosity (550 cps, at 30 ˚C) which facilitated improved handling. Several inks were dispensed and cured on different SL substrates and the E1660 ink (Ercon Inc., Wareham, MA) was selected for this research based on low average volume resistivity (2.7 x 10-7 Ω-m or 27 μΩ-cm, see Figure 3) across all substrates, curing temperature, and adequate viscosity for dispensing narrow, uniform, and high aspect ratio DP conductive traces (Lopes *et al.*, 2006).

The entire circuit was designed in the form of an assembly using SolidWorks® CAD design software and included the receptacles into which the corresponding electronic components were inserted. Figure 1.5 depicts the progression of the 2D 555 timer circuit fabricated within the hybrid SL/DP system and the details of the entire fabrication process are explained in Lopes *et al.* (2006). Specifically, the SL/DP process was initiated by building the SL base with the required sockets and vias for inserting the electronic components. Once a predetermined build stage was reached, the build was interrupted, the vat was lowered without raising the platform to expose the top surface, and the sockets and vias were cleaned using iso-propyl alcohol, as seen in Figure 1.5a. The components were then manually inserted into their respective sockets and vias while ensuring that the connector pins of the components were one layer thickness (0.004") below the last built layer to allow regular Zephyr™ blade sweeping when the SL build continued. After the components were inserted, the resin level was re-adjusted and the build was continued to embed the components. Here, the components were embedded while providing access to the connector pins of the electronic components via precise access holes manufactured during the SL build as seen in Figure 1.5b. The DP syringe was then directed to move to the starting point of the DP trace and LabVIEW® was used to guide the traverse system as well as

control the dispensing for completing the required interconnects using the DP system. The traverse sequence (which is a set of simple motion commands) was initiated, and the dispensing was controlled to start and stop as and when necessary to complete the entire DP circuit in one sequence.

After the ink deposition was complete, the functional part was removed from the machine, cleaned using iso-propyl alcohol, and cured in a standard heat convection oven. To test the effectiveness of the laser cured ink, the resistivity of the functional test piece was measured. The curing process was continued until the resistivity reached the value recommended by the ink manufacturer (25.4 μΩ-cm). It was found that curing at 80 °C for 2 hrs produced the required resistivity value. The total time for manufacturing the completed part with embedded components and DP interconnections was approximately three and a half hours.

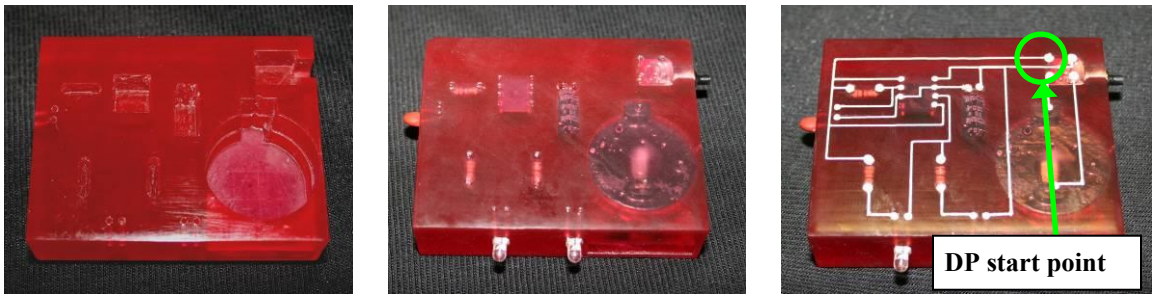

(a) **(b)** **(c)**

Figure 1.5. (a) SL part with sockets; (b) Embedded components; (c) DP interconnects

In summary, the second generation hybrid SL/DP system was utilized to fabricate electronics structures with embedded electronics and DP interconnects. The ability to utilize different materials and build complex geometries using the hybrid SL/DP system helped enable the design and manufacture of compact, visually appealing 3D circuits. By having components embedded within the design, they are protected from outside hazards and weather which increase the overall strength and reliability of the final product. As part of advancing this research, a

precise manufacturing process that can enable 3D structural electronic fabrication and help achieve significant size reductions as compared to current fabrication technique was investigated.

1.3 Fabrication Issues and Motivation for this Research:

The previous research demonstrated potential to fabricate 3D structural electronic devices, however, several manufacturing and design issues need to be addressed to achieve this goal. Although, this research demonstrated the use of the SL laser for curing the silver conductive ink dispensed during the manufacturing process, the substrate was severely charred. Thus, there was a need to determine the minimum laser energy required to effectively cure the ink. An extensive study was needed to fully understand the laser curing process. As part of this experiment, several laser parameters including laser power, scanning speed, scanning locations, and laser energy, need to be analyzed. The results from these experiments would help determine the laser parameters needs for the most effective laser ink curing condition. Also the curing profile width was higher than the actual trace width to compensate for registration errors. To eliminate this issue, the concept for fabricating accurately placed channels within the SL part into which the inks can be dispensed, was explored as part of this research. Additionally, several manufacturing issues can be foreseen for extending the 2D 555 timer fabrication concepts into 3D. These issues require investigations into improved circuit design and interconnect layout, optimum vertical interconnections between components and multiple routing layers based on complexity, temperature and energy control during laser curing of conductive inks and its effect on the electronic components, and heat dissipation when using high speed passive components operating at high frequencies.

With this motivation, SL and DP were combined in a single hybrid manufacturing system to provide an automated manufacturing environment for developing unique, freeform packages

with embedded 3D Structural Electronics (Lopes *et al.*, 2010). The structural component was fabricated using SL and the DP was utilized to complete the required interconnections between the embedded electronic components. The next sections describe the developments that have culminated into a fully integrated system and a corresponding manufacturing process that enables fabrication of complex, 3D structural electronic devices within a single integrated manufacturing environment.

1.4 References:

Chrisey, D.B. and Pique, A. (2002), *Direct-Write Technologies for Rapid Prototyping Applications: Sensors, Electronics, and Integrated Power Sources*, Harcourt Inc.: Academic Press, San Diego, California.

Jacobs, P.F. (1992), *Rapid prototyping & Manufacturing: Fundamentals of stereolithography*, Published by Society of Manufacturing Engineers, Dearborn, Michigan.

Kataria, A. and Rosen, D.W. (2001), "Building around inserts: methods for fabricating complex devices in stereolithography", *Rapid Prototyping Journal,* Vol. 7 No. 5, pp. 253-261.

Malone, E. and Lipson, H. (2006), "Freeform fabrication of ionomeric polymer-metal composite actuator", *Rapid Prototyping Journal*, Vol. 12 No. 5, pp. 244-253.

Medina, F., Lopes, A.J., Inamdar, A., Hennessey, R., Palmer, J., Chavez, B., Davis, D., Gallegos, P. and Wicker, R.B. (2005b), "Hybrid manufacturing: integrating stereolithography and direct write technologies", *Proceedings of the 16th Annual Solid Freeform Fabrication Symposium*, University of Texas at Austin, Austin, TX, pp. 39-49.

Lopes, A.J., Navarrete, M., Medina, F., Palmer, J., MacDonald, E. and Wicker, R.B. (2006), "Expanding rapid prototyping for electronic systems integration of arbitrary form",

Proceedings of the 17th Annual Solid Freeform Fabrication Symposium, University of Texas at Austin, Austin, TX.

Lopes, A.J., MacDonald, E. and Wicker, R. (2010), "Integrating stereolithography and direct print technologies for 3D structural electronics fabrication", *Rapid Prototyping Journal*, Accepted.

Palmer, J.A., Yang, P., Davis, D.W., Chavez, B.D., Gallegos, P.L., Wicker, R.B. and Medina, F.R. (2004), "Rapid prototyping of high density circuitry", *Rapid Prototyping & Manufacturing 2004 Conference Proceedings*, Rapid Prototyping Association of the Society of Manufacturing Engineers, Hyatt Regency Dearborn, Michigan. Also, *SME Technical Paper TP04PUB221* (Dearborn, Michigan: Society of Manufacturing Engineers).

Pique, A., Mathews, S.A., Pratap, B., Auyeung, R.C.Y., Karns, B.J. and Lakeou, S. (2006), "Embedding electronic circuits by laser direct-write", *Microelectronic Engineering*, Vol. 83, pp. 2527-2533.

Weiss, L. and Prinz, F. (1998), "Novel applications and implementations of shape deposition manufacturing", *Naval Research Reviews, Office of Naval Research, Three*, Vol. L.

Young, D., Sampath, S., Chikov, B. and Chrisey, D.B. (2005), "The future of direct writing in electronics", *CircuiTree.*

Chapter 2

2 RESEARCH OBJECTIVES

This main goal of this research was to develop an automated manufacturing environment that combines stereolithography (SL) and direct print (DP) in a single hybrid system for fabricating functional 3D structural electronic devices. This research evaluates the feasibility of combining SL and DP into a single hybrid functional system and analyzes the specific requirements associated with the integration of the two technologies. The various fabrication steps required for 3D structural electronics fabrication will be analyzed to determine the most effective and efficient manufacturing process. This research advances the concepts of integrating additive manufacturing (AM) and DP for producing functional, monolithic 3D structures with embedded electronics.

The specific objectives of this research are:

1. Characterization and selection of the SL resin and DP conductive inks
2. Characterization of the *in situ* UV laser ink curing process
3. Fabrication of functional 2D and 3D embedded electronic systems

The first objective analyzes important parameters for optimizing the selection of various SL and DP materials that facilitate fabrication of 3D structural electronic devices. The second objective examines the various parameters for successful *in situ* UV laser curing of particulate silver-based inks to determine the laser curing condition that resulted in the most effective ink curing. The third objective evaluates the fabricated 2D and 3D electronic devices for functionality. Overall, these objectives will advance the applications for AM technologies and present a new methodology for manufacturing non-traditional electronic systems in arbitrary form, while achieving miniaturization and enabling rugged structure.

Chapter 3

INTEGRATING STEREOLITHOGRAPHY AND DIRECT PRINT TECHNOLOGIES FOR 3D STRUCTURAL ELECTRONICS FABRICATION

The material for this chapter is from the paper titled ‗Integrating Stereolithography and Direct Print Technologies for 3D Structural Electronics Fabrication', which has been accepted for publication in the Rapid Prototyping Journal, by Emerald Group Publishing. The author would like to thank the Rapid Prototyping Journal for giving permission to include the material as part of this dissertation.

3 INTEGRATING STEREOLITHOGRAPHY AND DIRECT PRINT TECHNOLOGIES FOR 3D STRUCTURAL ELECTRONICS FABRICATION

Amit J. Lopes, Eric MacDonald, and Ryan Wicker

The University of Texas at El Paso, El Paso, Texas, USA

Abstract

Purpose *–A hybrid manufacturing system that integrates stereolithography (SL) and Direct Print (DP) technologies to fabricate three-dimensional (3D) structures with embedded electronic circuits is presented. A detailed process was developed that enables fabrication of monolithic 3D packages with electronics without removal from the hybrid SL/DP machine during the process. Successful devices are demonstrated consisting of simple 555 timer circuits designed and fabricated in 2D (single layer of routing) and 3D (multiple layers of routing and component placement).*

Design/methodology/approach *– A hybrid SL/DP system was designed and developed using a 3D Systems SL 250/50 machine and an nScrypt micro-dispensing pump integrated within the SL machine through orthogonally-aligned linear translation stages. A corresponding manufacturing process was also developed using this system to fabricate 2D and 3D monolithic structures with embedded electronic circuits. The process involved part design, process planning, integrated manufacturing (including multiple starts and stops of both SL and DP and multiple intermediate processes), and post-processing. SL provided substrate/mechanical*

structure manufacturing while interconnections were achieved using DP of conductive inks. Simple functional demonstrations involving 2D and 3D circuit designs were accomplished.

Findings *– The 3D micro-dispensing DP system provided control over conductive trace deposition and combined with the manufacturing flexibility of the SL machine enabled the fabrication of monolithic 3D electronic structures. To fabricate a 3D electronic device within the hybrid SL/DP machine, a process was developed that required multiple starts and stops of the SL process, removal of uncured resin from the SL substrate, insertion of active and passive electronic components, and DP and laser curing of the conductive traces. Using this process, the hybrid SL/DP technology was capable of successfully fabricating, without removal from the machine during fabrication, functional 2D and 3D 555 timer circuits packaged within SL substrates.*

Research limitations/implications *– Results indicated that fabrication of 3D embedded electronic systems is possible using the hybrid SL/DP machine. A complete manufacturing process was developed to fabricate complex, monolithic 3D structures with electronics in a single set-up, advancing the capabilities of Additive Manufacturing (AM) technologies. Although the process does not require removal of the structure from the machine during fabrication, many of the current sub-processes are manual. As a result, further research and development on automation and optimization of many of the sub-processes are required to enhance the overall manufacturing process.*

Practical implications *– A new methodology is presented for manufacturing non-traditional electronic systems in arbitrary form, while achieving miniaturization and enabling rugged structure. Advanced applications are demonstrated using a semi-automated approach to SL/DP integration. Opportunities exist to fully automate the hybrid SL/DP machine and optimize the manufacturing process for enhancing the commercial appeal for fabricating complex systems.*

Originality/value *– This work broadly demonstrates what can be achieved by integrating multiple AM technologies together for fabricating unique devices and more specifically demonstrates a hybrid SL/DP machine that can produce 3D monolithic structures with embedded electronics an printed interconnects.*

Keywords*: 3D structural electronics, Rapid prototyping, Integrated additive manufacturing, Direct write, Multiple materials*

Paper type*: Research paper*

3.1 Introduction:

The development and fabrication of Integrated Circuits (IC) and electronic devices continually present new opportunities for manufacturing innovation. Traditional IC manufacturing consists of a Printed Circuit Board (PCB), which interconnects electronic components using flat conductive traces laminated onto a non-conductive substrate. However, PCB manufacturing processes have inherent waste of materials and are not environmentally friendly due to the required chemical processes (Mosses and Brackenridge, 2003). Furthermore,

the electronic components on a PCB need to be placed in a planar array on the board leading to reduced placement freedom and increased space requirements. Embedding electronic circuits within geometrically-complex substrates at various depths can enable substantial reductions in volume and weight. The Mesoscopic Integrated Conformal Electronics (MICE) program, developed at the Defense Advanced Research Projects Agency (DARPA), provided a platform for fabricating electronics, sensors, and antennas on conformal surfaces including helmets and other wearable gear for applications in harsh environments. This technology platform, originally referred to as Direct Write (DW) and more recently as Direct Print (DP), refers to any technique capable of depositing, dispensing, or processing a variety of materials over different surfaces in a preset pattern (Chrisey and Pique, 2002), and the DARPA MICE program (1999 - 2001) resulted in considerable advancements in DP. However, the capabilities of using traditional Additive Manufacturing (AM) or Rapid Prototyping (RP) technology for these applications have not been explored in the context of fabricating and prototyping complex electronics in which conformal, intricately-detailed shape, rugged/light-weight integration, and a natural resistance to reverse engineering are paramount.

The key concept of AM is layer-based additive manufacturing of 3D parts from digital data, which allows design flexibility, complex parts with provisions for prompt design changes, and mass customization. AM, however, was developed primarily to provide prototypes to be used in the design and production processes and not as a direct part production tool. As a result, AM technologies have been typically confined to single build materials with a constrained build envelope (in size and environment) and limited to the stacking of individual layers that precludes conformal printing. Despite these potential restrictions, researchers have widely explored using AM technologies for building functional products (Kruth *et al.*, 1998; Cham *et al.*, 1999; Doreau

et al., 2000; Palmer *et al.*, 2004; De Laurentis and Mavroidis, 2004; Robinson *et al.,* 2006; Chartier *et al.*, 2008; Czajkiewicz Z., 2008; Wohler's Report, 2010), including research on processes capable of building with multiple materials (Weiss *et al.*, 1997; Inamdar *et al.*, 2006; Janaki Ram *et al.*, 2007; Malone *et al.*, 2007). It was during these developments that the concepts for integration of AM and DP for producing functional, monolithic 3D structures with embedded electronics emerged.

One important advancement in AM was demonstrated by Kataria and Rosen (2001) where stereolithograhy (SL) was used to embed functional inserts by implementing a start and stop process during the build. This research inspired the concept of embedding virtually any component including electronics within an SL matrix by utilizing the advantages of the SL system. As part of the DARPA MICE program described above, Church *et al.* (2000) utilized an advanced micro-dispensing DP system to print conductive lines onto glass substrates for creating wireless sensor systems. DP manufacturing complements the field of AM and can be used to fabricate passive 3D structures and functional prototypes (Young *et al.,* 2005). It was only natural for the work of Kataria and Rosen (2001) to be combined with Church *et al*. (2000) to utilize the combined advantages of SL and DP in a single integrated manufacturing environment to build rugged, arbitrarily-formed electronic systems.

The integration of SL and DP technologies for the fabrication of 3D, high-density circuitry has evolved over a number of years (Palmer *et al.*, 2004, 2005; Medina *et al*., 2005a, 2005b; Lopes *et al.*, 2006; Navarrete *et al.*, 2007; DeNava *et. al.*, 2008; Muse *et. al.*, 2009), and the developments have resulted in a process that can build 3D electronic structures within the hybrid SL/DP machine without removal of the part during fabrication. Early developments (Palmer *et al.,* 2004, 2005 and Medina *et al.*, 2005a) demonstrated the feasibility of rapidly

manufactured functional electronic systems using DP and SL in separate processes by exchanging the part between machines. As time advanced in the development, improvements in both the SL/DP process and an increased level of sophistication of the integrated electronics have been achieved. Medina *et al.* (2005b) and Lopes *et al.*, (2006) used an early version of the hybrid SL/DP machine to fabricate simple circuits. Lopes *et al.* (2006) fabricated a simple 2D 555 timer circuit and demonstrated the feasibility for manufacturing electronic systems with embedded components using the hybrid machine although the interconnects was designed to be printed in a 2D layout on a single layer. A similar LM555 timer circuit was independently demonstrated by Pique *et al.* (2006) on a polyetherimide substrate using a different DP process called laser direct write (LDW) in which a laser was used for micromachining (subtractive) as well as controlling the amount of conductive material transferred to the substrate (additive). This work developed a complete process for fabricating embedded electronic systems in polyetherimide, describing a number of advantages associated with (1) embedding electronic components, (2) using the substrate as both the circuit board and electronics packaging, (3) maintaining processing temperatures below ~100 ^{o}C, allowing the process to be extended to a variety of plastics as substrates, and (4) fabricating 3D component and circuit layouts to improve utilization of 3D volumes.

Although not conventional AM technology, the work described in Pique *et al.* (2006) served to motivate further improvements to the hybrid SL/DP manufacturing process, and Navarrete *et al.* (2007) introduced channels into the substrate during SL fabrication for the conductive material in order to provide delineation of the electrical lines and allow for the reduction of line pitch, width and spacing while reducing the possibility of line-to-line shorting. Line spacing was thus controlled by the precision of the SL fabrication (e.g. laser beam size and

resin polymerization characteristics) rather than the dispensing process. DeNava *et al.* (2008) described a 3D electronics device that included off-axis component placement and routing for a 3D magnetic flux sensor with microcontroller, as shown in Figure 3.1, illustrating the reductions in size of the electronics package afforded through 3D placement of components and routing of conductive traces. Castillo *et al.* (2009) extended this concept to a truly conformal application in which an accelerometer, microprocessor and wireless subsystem were created within an insert that was designed to conform to the interior of a helmet in order to detect and wirelessly report traumatic head injury. This work included a unique functional conformal antenna fabricated with AM. These developments have culminated into the current work that describes a fully integrated system and process that enables fabrication of complex, 3D structural electronic devices within a single integrated manufacturing environment - called 3D Structural Electronics since mechanical structures and electronics are integrated in a single, monolithic package.

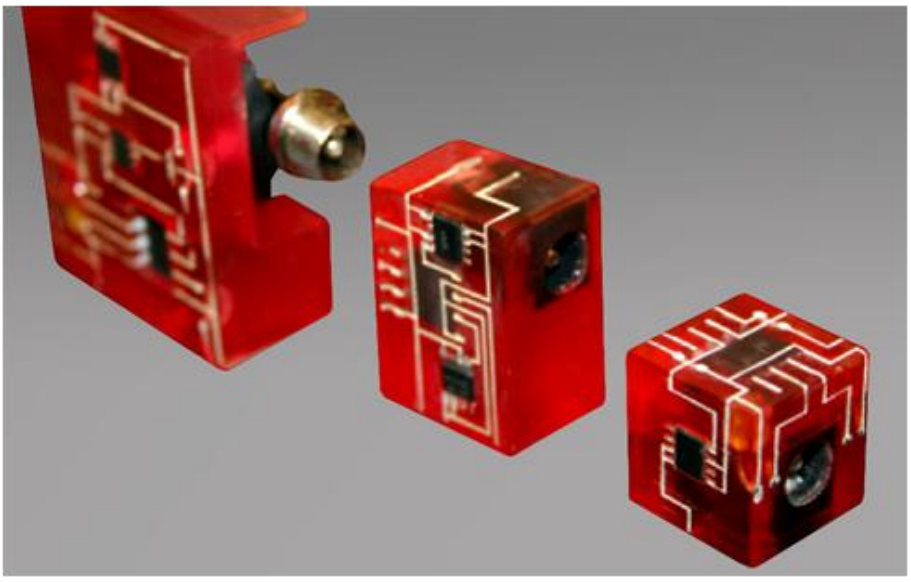

Figure 3.1. Three Generations of a Three-Axis Magnetic Flux Sensor System

Using AM technologies to fabricate 3D Structural Electronics is not unique to SL and several other researchers have been exploring other AM technologies to accomplish similar

goals. Early pioneering work in structural electronics fabrication was demonstrated by Weiss and Prinz (1998) and Cham *et al.* (1999) where they utilized the shape deposition manufacturing technology to integrate electronic components and interconnects in a urethane structure to form a waterproof wearable computer with embedded electronics. Robinson *et al.* (2006) integrated DP ink dispensing and Ultrasonic Consolidation (UC) technologies to manufacture electronic circuitry, antennas and other devices directly into a solid metal structure fabricated in UC. Malone and Lipson (2006) used the Fab@Home AM machine to fabricate ionomeric polymer-metal composite actuators through the development of novel material formulations. Malone *et al.* (2007) and Periard *et al.* (2007) further demonstrated manufacturing flexibility of the Fab@Home machine by fabricating multi-material, functional Zn-air batteries, a LM555 timer circuit similar to that demonstrated in Lopes *et al.* (2006) and Pique *et al.* (2006) as well as several clever electro-mechanical applications. The access to individual layers while a 3D object is additively fabricated enables virtually any AM process, such as 3D printers using jetting technologies, fused deposition modeling machines, laser sintering machines, and other AM systems, to be candidates for fabricating 3D structural electronic devices. There are, however, a number of challenges associated with each technology in order to stop and start the process for component insertion, ensure that the inserted components do not interfere with the AM processes (i.e., the material dispensing or recoating mechanisms may crash into an inserted component), and are compatible with integrating direct printing of conductive traces or some other method of introducing conductive interconnect. Controlling the build process in commercial AM systems is especially difficult since system manufacturers generally do not provide access to the control software to modify the build sequence or toolpaths. However, it would be natural to expect additional AM technologies to be explored by researchers and AM system manufacturers as the

benefits of building 3D structural electronic systems using AM are more fully exploited and the commercial opportunities for these devices become realized.

As illustrated in Figure 3.1 and the above discussion, there are clear advantages in 3D electronics packaging afforded by AM. As a result, this research describes the development of an automated manufacturing environment that combines SL and DP in a single hybrid manufacturing system to capitalize on each individual process capability for developing unique, freeform packages with embedded components for 3D structural electronic systems. The focus of this research was to develop the hybrid system for fabricating 3D circuits to achieve significant miniaturization wherein components were embedded at different depths and orientations within the substrates, requiring a variety of multi-dimensional interconnections between components. This new 3D Structural Electronics approach represents a possible paradigm shift in traditional PCB manufacturing. The following describes the developed hybrid SL/DP system and the manufacturing processes required to fabricate monolithic 3D structural electronic devices. A simple parametrically-sensitive circuit similar to those demonstrated previously by Lopes *et al.* (2006), Pique *et al.* (2006), and Periard *et al.* (2007) was selected to evaluate the effectiveness of the hybrid SL/DP system for manufacturing structural electronics designed and demonstrated in both 2D (single layer of routing) and 3D (multiple layers of component placement and routing). Finally, several additional advanced electronics applications, which were fabricated with AM but not in an automated fashion, are described to illustrate the potential of this new electronics fabrication technology.

3.2 Systems and Materials:

3.2.1 SL System

Line-scan stereolithography (SL), a three-dimensional layer-based additive manufacturing process that builds parts by scanning a laser beam across a vat of liquid photopolymer and stacking individually cured layers on top of one another, was selected as the freeform fabricator for this research. SL provides superior dimensional accuracy and surface finish compared with many other commercially available AM technologies and provides several advantages for integration with other manufacturing technologies due to the ease of access to the build chamber, flexible optics, high accuracy fabrication capabilities, and a variety of available build materials. However, the primary reasons for selecting SL as the base AM system in this research were the ability to start and stop the build at any given layer as well as a simple ambient build chamber (i.e., SL essentially requires no control over the build environment other than a UV protective enclosure). These SL system advantages enabled a straightforward integration of a DP system with the SL system so that mechanical structures could be fabricated simultaneously with integrated and functional electronic systems. The commercial SL system selected for integration was a 3D Systems 250/50 SL machine (3D Systems, Rock Hill, SC) equipped with a 355 nm solid-state laser upgrade (Series 3500-SMPS, DPSS Lasers Inc., Santa Clara, CA).

3.2.2 DP System

Direct Print (DP) refers to any technique capable of depositing, dispensing, spraying or transferring by some means a variety of materials onto a surface in a preset pattern captured in a digital file (Chrisey and Pique, 2002). DP provides precision controlled on-demand dispensing of functional materials for a variety of applications. For this research an advanced nScrypt Smart

Pump™ 100 (nScrypt, Inc, Orlando, FL) system capable of dispensing lines having 25 micron line widths at speeds of 250 mm per second was selected as the micro-dispensing tool (nScrypt, Inc, 2010). The Smart Pump™ 100 can dispense very small volumes of material (10^5 μm^3) over a wide range of viscosities (0.001 Pa-s to 1,000 Pa-s) to enable the printing of complex structures with small feature sizes and enhanced degrees of control (nScrypt, Inc, 2010). The SmartPump™ 100 can control the dispensing pressure from 0-6.894×10^5 Pa (0-100 psi) with ~690 Pa (0.1psi) resolution. The precise dispensing control enables printing of complex designs with accurate corners (i.e., line widths), and based on the above specifications, was selected as the DP system to be integrated with the SL machine.

3.2.3 SL/DP Integration

When the manufacturing flexibility of the SL process is combined with the 3D micro-dispensing capability of the nScrypt Smart Pump™ 100 system, unique monolithic 3D packages with embedded electronics can be fabricated in a single manufacturing process. The developed hybrid SL/DP machine is shown in Figure 3.2.

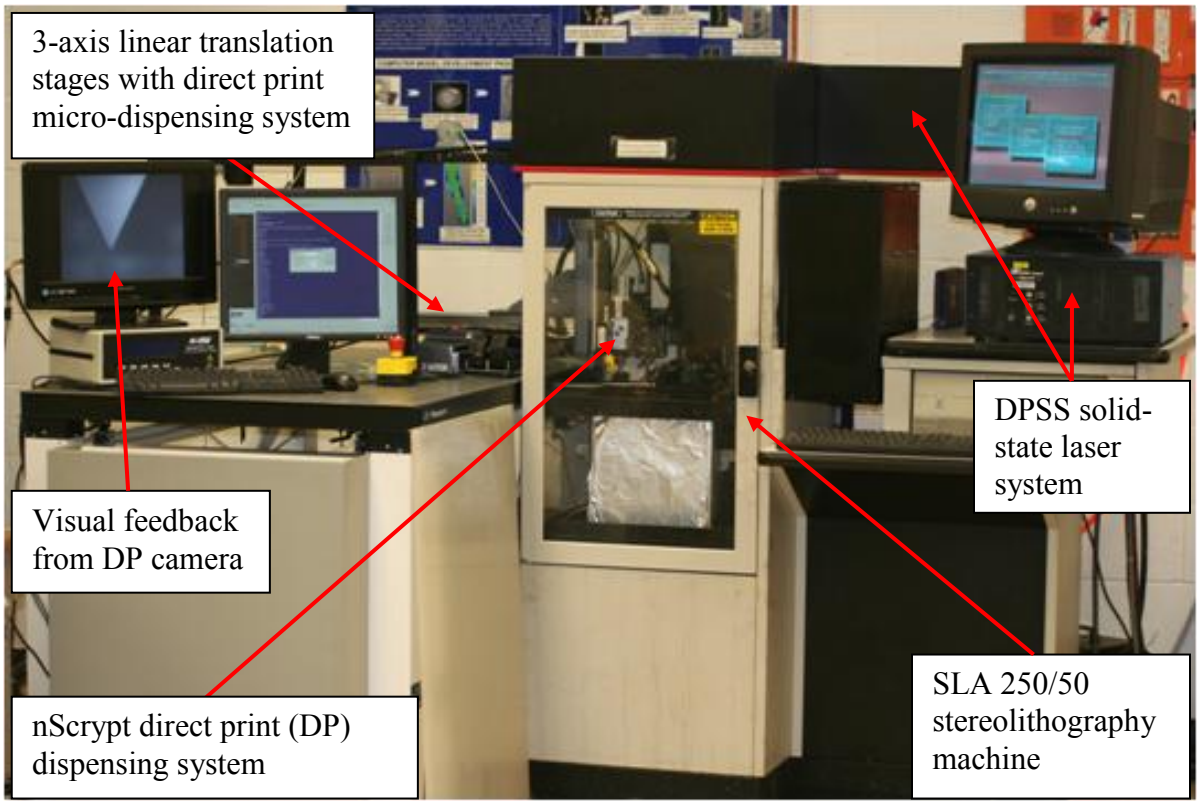

Figure 3.2. The hybrid SL/DP machine

3.2.3.1 Hardware

The hybrid SL/DP machine (Figure 3.2) represents a simple integration of the separate SL and DP systems and the basic configuration of the hybrid system has been described in several previous publications (Lopes *et al.*, (2006); Navarrete *et al.*, (2007); DeNava *et al.* (2008); Castillo *et. al.* (2009)). Briefly, the side wall of the SL enclosure was removed to provide access for the DP dispensing system to the build chamber. The DP pump was attached to orthogonally-aligned precision linear positioning stages (Parker Hannifin Corporation, Electromechanical Automation Division, Rohnert Park, CA) placed on a standard 61 cm x 122 cm research grade Newport honeycomb breadboard (Newport Corporation, Mountain View, CA). The entire DP setup was placed on an adjustable-height hand-crank two-legged mobile

workbench (Part # 9054T113 and Part # 3517T82, respectively, McMaster-Carr Supply Company, Chicago, IL) and a UV protective enclosure (UF-3/4, Baker Glass/Baker Plastic, El Paso, TX 79903) was built around the DP system. The nScrypt Smartpump^{TM} 100 was attached to the Z-stage of the 3-axis linear positioning system such that the dispensing nozzle tip was perpendicular to the SL part. The DP set-up included a camera (68 mm InfiniStix^{TM}, Infinity Photo-Optical Company, Boulder, CO) focused on the dispensing nozzle to provide the operator with visual feedback of the dispensing process.

3.2.3.2 Software

The linear positioning system (stages) as well as the dispensing system were controlled with a custom DP control program written in an assembly language script that was used to communicate with the control software of the stages and the nScrypt Smart Pump™ 100 DP dispensing system. The DP control system was connected to the stage control system via a serial communication port. The custom DP script (control program) was used to control both systems simultaneously to achieve accurate and simultaneous motion along three axes coupled with on-demand dispensing. The DP script provided real-time control over the dispensing pressure and traverse speed to enable precision dispensing of the conductive media used as conductive electronic traces.

3.2.4 Materials

Several candidate SL resins (as described in Lopes *et al.*, 2006) were previously investigated for use as SL substrates to be used in 3D structural electronic devices. Characteristics considered in the selection of the resin included dielectric nature, an ability to withstand high temperatures required to cure the candidate inks and low viscosity for easier

cleaning during fabrication. Of the candidate resins, the ProtoTherm™ 12120 (DSM Somos®, Elgin, IL) resin was selected due to its ability to withstand relatively high temperatures (e.g., heat deflection temperature of 126.2˚C after a thermal postcure treatment, measured at 0.46 MPa as per ASTM D648-98c) required to cure the inks, and relatively low viscosity (0.550 Pa-s at 30˚C) that enabled improved handling and cleaning – all of which facilitated the fabrication of embedded electronic systems (ProtoTherm™ 12120 Product Data Sheet, DSM Somos, Elgin, IL). The focus of current research with regard to materials for structural electronics applications includes ceramic-based stereolithography, micro-stereolithography and 3D printing as ceramic materials provide superior dielectric properties (Doreau *et al*., 2000, Chartier *et al.*, 2008).

The fabrication of electronic systems through printing techniques such as direct print, inkjet, and rotogravure are made possible through the utilization of particle-based conductive inks. Metals that have been used in conductive ink applications include gold, silver, copper, and nickel (Jagt, 1998), and these metals have been used as micro-scale particles and flakes with increasing emphasis on the synthesis of nano-particles for use in these conductive inks. Much research has been invested in ink development, and the interested reader is referred to (Mo *et al.,* 2009; Park *et al.,* 2007; Pudas *et. al.,* 2005) for additional information. To enable the integration of SL and DP processes, inks with low processing temperatures which can be easily and accurately dispensed were preferred. Several silver-based candidate inks were selected for testing with curing temperatures that ranged from 110 – 138˚C (see Table 3.1). The limitations on ink curing temperature were imposed by the maximum storage temperature of the electronic components used in the circuits, typically ranging from 85˚C to 150˚C, and the temperature limitations imposed by the SL resin. Previous work (Lopes *et al.*, 2006) tested several inks on SL substrates and the E1660 ink (Ercon Inc., Wareham, MA) was selected based on low average

volume resistivity (2.7 x 10^{-7} Ω-m or 27 μΩ-cm, see Figure 3.3) across all substrates, curing temperature, and adequate viscosity for dispensing narrow, uniform, and high aspect ratio DP conductive traces.

Table 3.1. Conductive inks for the direct print process.

Manufacturer	Ink	Conductive Particulate Material	Viscosity (Pa-s)	Volume Resistivity (μΩ-cm)	Cure Temp (°C)	Time (Minutes)
EMS Far East Ltd.	CI-1001	Silver	12	< 38	110	10
EMS Far East Ltd.	CI-1002	Silver	7.5	< 89	110	10
Ercon Inc.	E1400	Silver	15	12.7 - 30.48	138	15
Ercon Inc.	**E1660**	**Silver**	**18.75**	**12.7 - 30.48**	**138**	**15**
Advanced Conductive Materials	PT10-A	Silver	12.5	< 38	110	15
Paralec	Parmod® VLT silver	Silver	17.46	10-14	140-150	3-8
NA	Bulk Silver	Silver	N/A	1.59	N/A	N/A

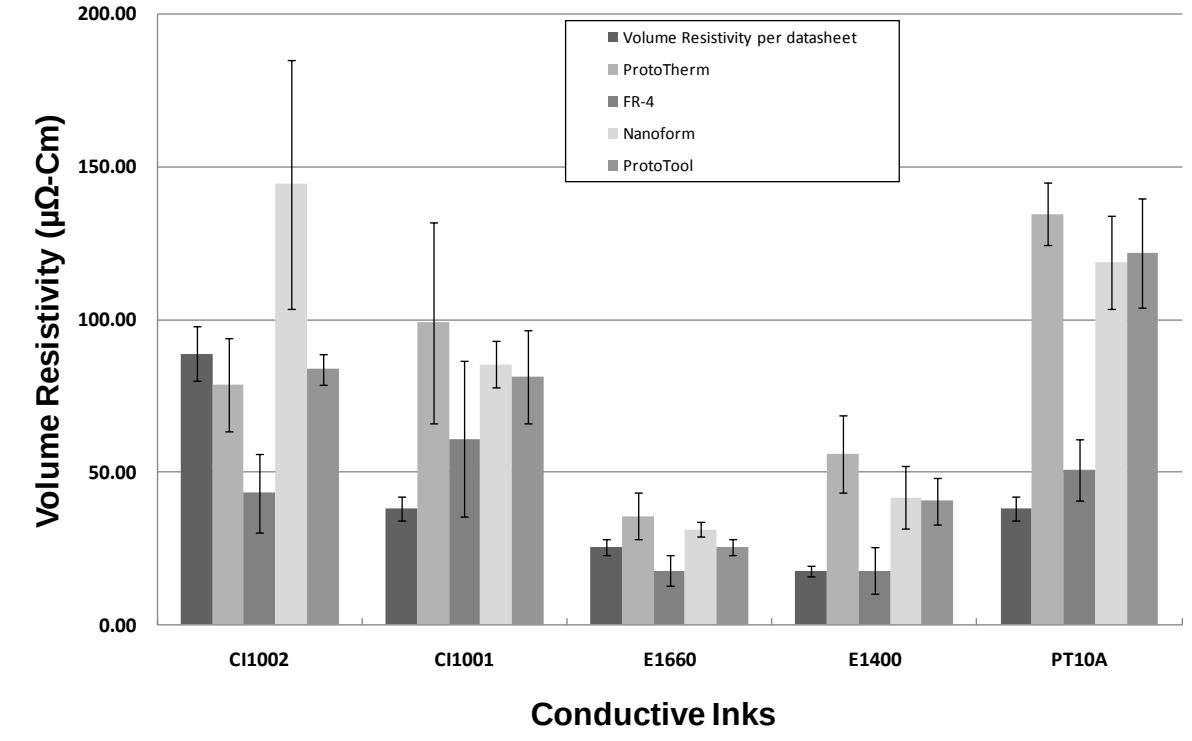

Figure 3.3. Comparison of volume resistivities of various inks on different substrates

(Error bars represent ± 1 standard deviation; n=5)

3.3 Fabrication Design and SL/DP Process Overview:

To fabricate a 3D structural electronic device within the hybrid SL/DP machine without removal of the device from the machine during fabrication, a process was developed that required multiple starts and stops of the SL process, uncured resin removal from the SL substrate, insertion of active and passive electronic components, DP and then laser curing of the conductive traces. The general manufacturing process diagram for this process is shown in Figure 3.4. Briefly, these steps include SL part design using CAD, part preparation using 3D Lightyear^{TM} software, build process planning for 3D fabrication without part removal, SL fabrication, SL process interrupt with uncured resin removal and cleaning from the SL substrate, component insertion, SL process start for component embedding, SL process interrupt and uncured resin removal and cleaning for DP, DP/SL registration, DP, and ink curing. These SL / cleaning / component insertion / DP / ink curing processes are continued as necessary to fabricate 3D electronic devices with multiple layers and components. Once the build is completed, the part undergoes final cleaning, final cure, and test for functionality. Additional details for the individual processes are contained in the following section.

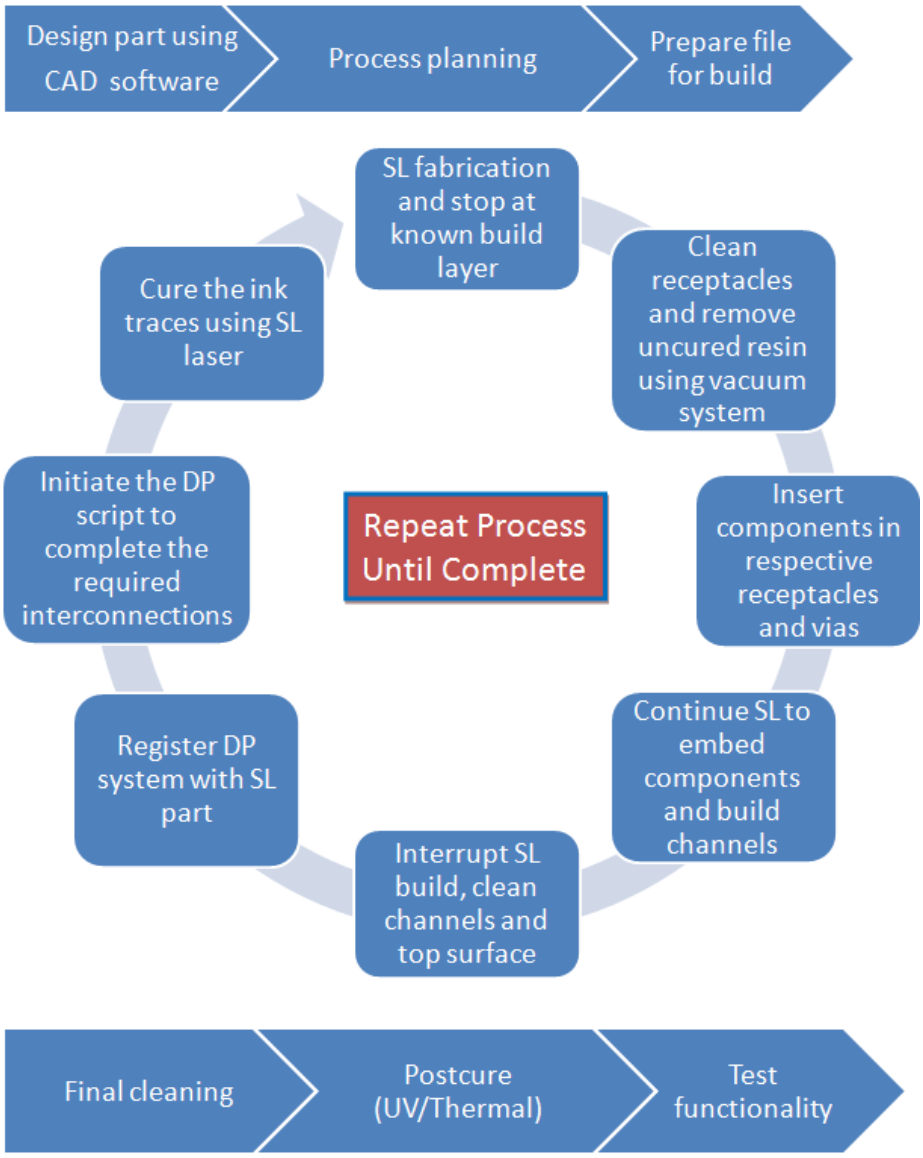

Figure 3.4. The general embedded electronics fabrication process cycle

3.3.1 CAD Design and Part Preparation

An entire build is designed using any CAD design software, saved as a part file, and converted into a _.stl‘ file. The receptacles for the components are arranged so as to minimize the volume of the circuit and to simplify the DP interconnections. The component with the most pins is generally placed at the center and the remaining components are arranged around it to

ensure the most concise circuit design. In 3D designs, the largest components are embedded first to minimize the number of vertical vias required and reduce the overall size of the final circuit. Furthermore, channels are incorporated into the design to contain the DP ink and provide control over the trace widths and to assist in vertical via alignment during the 3D fabrication process. Using these guidelines, the designs in this work were placed manually. Although many algorithms and software are available for component placement and routing in 2D electronics, a need exists for extending and implementing these algorithms in 3D.

The _.stl‘ file is utilized to generate the 2D slices of the 3D part in 3D Lightyear™ software and prepare the build files (four different files, each one with different information necessary to build the part). The vector (.v) file contains the entire build information in individual layers of ~100 μm (0.004”) thickness in the form of vectors (start and end point defined by X, Y, and Z coordinates) that are traced by the laser. The vector file is analyzed across all of the build stages of the part to plan the fabrication process by interrupting the build at known layers in order to embed electronic components, incorporate DP, and continue the build, if necessary.

3.3.2 Stereolithography

The fabrication process is initiated in SL by building the base of the part with the required receptacles into which the electronic components will later be press-fit, the channels that delineate the conductive ink trace, and the vertical vias for interconnection between multilayer electronic components. Once the base part is built, the SL process is paused to clean the receptacles, embed electronic components, or incorporate DP as necessary based on the design. SL can be resumed to continue the build as required.

3.3.3 SL Part Cleaning and Component Insertion

After the SL build is interrupted, the vat is lowered (~ 100mm using the _unload vat' command of the SL system) to expose the top surface of the SL part and clean the receptacles, vias, and channels using the resin manufacturer's recommended solvent. A vacuum system (Model No. 400-1901, Barnant Co., Barrington, IL) is also used for removing uncured resin and any remaining cleaning solution. Alternatively, the vacuum process can be performed on uncured resin without using the solvent followed by a scan of the UV laser system to cure any residual resin in the scanned regions. This process would avoid possible contamination of the resin by the solvent, but may result in dimensional inaccuracies due to curing un-removed uncured resin. However, contamination may be an issue to explore and this alternative approach as well as a variety of other strategies will be investigated in the future. In the current approach, once the cleaning process is complete, the substrate is populated with the necessary components using a manual component insertion approach - the automation of which is straightforward with pick and place PCB technology and is another useful subject for future work. The build is continued (1) to embed the electronic components while providing access to the connection pins or (2) to dispense the conductive traces using DP.

3.3.4 DP/SL Registration

The ability to accurately register the DP nozzle with the SL part and precisely dispense electrical interconnections using the DP system is essential for successful SL/DP integration. There are several methods to register between the SL substrate and the DP tip, including laser scanning of surface contours and 3D linear positioning systems, and any method can be used depending on required functionality. In the approach used here for registration, the dispensing nozzle tip is directed to a predetermined starting point, which can be a pin of an encapsulated

electronic component and the stand-off distance is adjusted using standard slip gauges. Current work is improving and automating the registration process.

3.3.5 Direct Printing

Electrical interconnections are created by precisely dispensing conductive material onto the SL substrate between the electronic components and within the SL channels. Here, a custom DP control program was used to guide the traverse system as well as control the dispensing for the DP interconnects using the nScrypt Smart Pump^{TM} 100 dispensing system. After the dispensing nozzle is aligned with the starting point, the traverse sequence (a set of simple motion commands replicating the DP profile) is initiated, and the dispensing is controlled to start and stop, as necessary, to complete the entire DP circuit in one sequence.

3.3.6 Conductive Trace Curing

Before continuing with the process and resuming the SL fabrication to embed the electronic components and conductive traces, the deposited ink should be cured *in situ* to avoid contamination between the ink and the SL resin when the substrate is submerged back into the vat of resin. In this work, the DPSS SL laser (355 nm) was utilized to cure the printed conductive traces. The laser power can be adjusted using the optical attenuator and the scan speed can be controlled by changing the depth of penetration (D_p) parameter. The dispensed conductive traces are patterned with the SL laser at 97.7 mW laser power and 482.6 μm/s scan speed to cure the ink. Once the ink is laser cured, the steps described above in Section 3.2 (Stereolithography) to Section 3.6 (Conductive Trace Curing) can be repeated as necessary until a complete 3D circuit is fabricated.

3.3.7 The Final Cleaning and Curing

After the complete device is fabricated, the final part is removed from the hybrid SL/DP machine to be cleaned using the recommended solvents. The part is then cured in a UV oven for 30 minutes on a side, and then baked in a standard heat convection oven at 80ºC for 2 hours to carry out the recommended thermal curing for the conductive ink. Finally, the part is inspected for any defects and tested for functionality.

3.4 Examination of *In Situ* UV Laser Curing of Silver-Based Conductive Ink:

As described above, to enable 3D component placement and routing, a sequence of processes were developed that included a sub-process for *in situ* intermediate UV laser curing (at 355 nm) of the conductive ink traces. Preliminary research demonstrated that the SL laser could be used to cure the ink sufficiently to continue the build without contamination between the ink and SL resin. By curing the conductive traces *in situ*, the construction of monolithic 3D structural electronic devices can be performed without removal of the device from the machine during fabrication. However, investigation into *in situ* laser curing was required to develop an effective and efficient procedure. As a result, the following three experiments were performed to explore the minimum number of laser passes required for simultaneously reducing interconnect resistance and manufacturing time.

3.4.1 Effect of Laser Power on Effective Curing Temperature during Laser Curing

In the hybrid SL/DP machine described here, the SL system does not have automated control over the DPSS solid-state laser power, although the laser power for this system can be adjusted manually using an optical attenuator integrated with the laser. This allows the laser power to be increased during ink curing, and thus can be used to reduce the time and number of laser passes required to cure the ink and continue with the SL build. To determine the effect of laser power on SL substrate temperature, a simple steady-state experiment was performed initially that related incident laser beam power to the corresponding steady-state substrate temperatures. The experiment also helped determine the laser energy absorption behavior of both the SL resin and the silver-based particulate ink. The experiment was carried out with a laser power of 97.7 mW, which is similar to the laser power used in the newer generation Viper si2 SL machine (3D Systems Inc., Rock Hill, SC) but greater than the typical ~50 mW used to

fabricate parts in the 250/50 SL machine. Operation above ~100 mW laser power could potentially damage the reflective surfaces on the scanning mirrors in the 250/50 SL machine, and thus, 97.7 mW was used as the maximum available laser power for ink curing. The amount of UV laser energy absorbed (measured as thermistor temperature) was measured with a 10 KΩ (@ 25°C) thermistor (NTCG103JF103FT1, TDK Corporation, Uniondale, NY) embedded in an SL test piece, where the effective steady-state temperature was calculated using the Beta equation (GE White papers, Thermometrics Inc, 2008). The thermistor resistance was measured using a Keithley 2000 series multimeter (Keithley Instruments Inc., Cleveland, OH) while focusing the laser on the thermistor at three different experimental conditions: (1) on the bare thermistor, (2) with two standard build layers (~203.2 μm) of cured SL resin on top of the thermistor, and (3) with an additional ~140 μm layer of uncured ink on top of the cured SL resin layer. Under these experimental conditions, the steady-state temperature measurements were 83°C for the bare thermistor, 75.5°C with the cured SL resin layer on top, and 47°C with the additional ink layer. The reflectivity of silver in the UV spectrum has been shown to be complex where it varies rapidly from ~0% at 316 nm to over 90% at 375 nm with a reflectivity of ~80% at 355 nm (Hecht, 2002). Although rapidly varying in the UV spectrum, the high reflectivity of silver at 355 nm may help explain the reduced energy absorption by the silver particles resulting in a lower measured thermistor temperature for this experimental condition. It should be noted that the corresponding steady-state temperatures for lower laser powers will be correspondingly lower than those for 97.7 mW where, for example, the measured temperature on the bare thermistor for a 77mW laser power was 63°C. Based on these results, the effect of the number of laser scans on ink resistance for scanning directly on the ink trace as well as next to the ink trace on the SL substrate were investigated. Scanning the SL substrate directly in close proximity to

the ink trace was explored to test if the increased energy absorbed by the SL substrate could potentially improve the ink curing process. These experiments are described in the next section.

3.4.2 Effect of Repetitive Laser Scanning on Trace Resistance

As described above, the silver particles in the ink or the ink solution appeared to reflect a significant amount of incident UV laser energy as shown through a reduced thermistor temperature when scanning directly on the ink versus on the SL substrate. Consequently, an examination of the effect of successive laser scans on trace resistance was conducted for both 1) scanning on top of the ink trace as well as 2) scanning on top of the SL resin in the vicinity of the trace. Ink curing typically involves a thermal oven curing process that includes solvent evaporation followed by curing of a resin binder that serves to bind the silver particles together. Details of the typical ink curing process and electrical resistivity measurements can be found in (Bieri *et al.*, 2003; Banfield, 2000). Experiments, similar to those presented here, are described in Fearon *et al.* (2007) for the effects of substrate type (conductive or non-conductive) on laser curing of silver based inks using 10.6 μm infrared laser energy. In the present experiments, the effects of repetitive UV laser scans were explored to determine the minimum number of laser scan passes required to effectively cure the ink so that the SL build could continue without contamination between the ink and SL resin. In addition to contamination, it was further desired to determine if laser curing could be used to reduce ink resistivity to that reported in the datasheet (E-1660 Product Data Sheet, Ercon Inc, Wareham, MA) and to determine if a final thermal post-cure was required at the end of the fabrication process. If required, it was uncertain what impact embedding the conductive traces in SL resin would have on the ink thermal curing process. As will be shown in the following section, the trace resistance could be successfully reduced after fabrication using the typical thermal oven curing process, and thus, a combined

procedure involving laser scanning of conductive traces to eliminate contamination during fabrication as well as a final thermal post-cure to minimize trace resistance was determined to be optimal in the fabrication of 3D structural electronic devices. In general, oven curing is preferred since it processes the entire system including multiple layers of conductive traces simultaneously, thus leaving the SL tool available for additional high value production. The details of an optimized procedure are left as future research.

In the current experiment, a sample test piece with four channels, 381 μm (0.015") wide, 406.4 μm (0.016") deep, and 11mm long, was fabricated using SL. The channel widths were chosen based on (1) contemporary PCB technology, which commonly uses conductors ranging from ~50 μm to 640 μm (0.002" to 0.025") in width, and (2) a reasonable channel width that could be fabricated using the typical laser beam diameter, ~250 μm (0.010"), of the 250/50 SL machine. The E1660 silver-based conductive ink (Ercon Inc., Wareham, MA) was deposited in the channels with an additional 1.0 mm on each side of the trace to make satisfactory connections to the copper pads, as shown in Figure 3.5(a). Four separate laser scanning _stl' files having width of ~250 μm (0.010") were created to replicate four different scan locations: (1) centered on the ink within the channel (called –on ink"), (2) ~190 μm (0.0075") from the center of the channel or centered on the edge of the substrate/ink interface (called –on edge"), (3) ~445 μm (0.0175") from the center of the channel (called –on SL substrate1"), and (4) ~570 μm (0.0225") from the center of the channel (called –on SL substrate2"). These scan locations are shown in Figure 3.5(b). The four separate laser curing _stl' files were utilized to cure the ink traces at 97.7 mW laser power with ~480 μm/s (0.019"/s) scan speed. Each test piece with the four channels was scanned with only one of the specific scan profiles (e.g., centered on ink) so that four resistance measurements were obtained and averaged for each

scanning condition. The laser pass took ~50 seconds to complete and was repeated 12 times to provide data for trace resistance as a function of the number of laser scan passes. The resistance across the trace was recorded three minutes after each laser pass using a Keithley 2000 series multimeter. Finally, to test the repeatability of the procedure, the laser curing experiment centered on the ink was performed first and then repeated after the other experiments for comparison. Results from these experiments are described below.

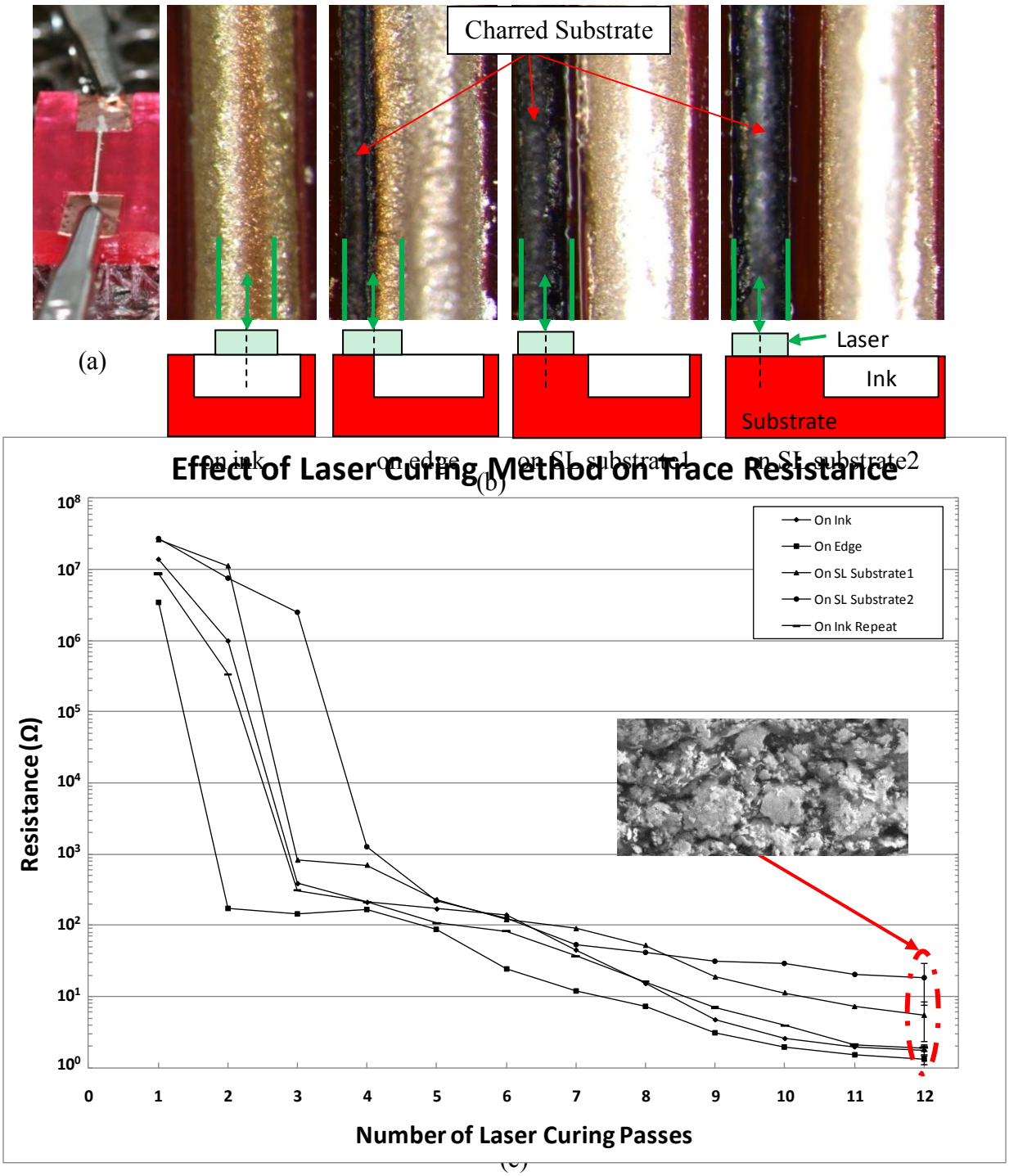

Figure 3.5. (a) Laser curing experiment set-up, (b) Samples (c) Effect of laser curing scan locations on trace resistance (SEM image of on ink sample after 12 passes) (Error bars shown at 12 laser passes represent ± 1 standard deviation; Error bars not shown at other laser curing passes for clarity; n=4)

The results of the laser scanning experiments are shown in Figure 3.5(c). As can be seen in the figure, all of the laser scanning conditions successfully reduced trace resistance, and these reductions continued to improve the resistance for each additional laser scan pass. There is evidence of two distinct curing phases that take place during cyclic laser curing. During the first phase (from one to four laser passes), there is a rapid reduction in trace resistance. This can be attributed to the rapid evaporation of the solvent material due to laser heating. In the subsequent phase (from the rapid evaporation phase up until the last laser scan pass), an asymptotically approaching steady-state resistance is being reached. In every case, the final trace appears to be a network of closely knit silver ink particles assisted by a proprietary binder material, as seen in Figure 3.5(c).

Further analysis of the data in Figure 3.5(c) shows that the laser curing profile at the scan location ―on edge" (~190 μm away from the center channel) provided the lowest measured trace resistance after 12 laser scan passes, followed by ―on ink", ―on SL substrate1" and ―on SL substrate2". As the laser beam scans farther away from the ink channel from ―on SL substrate1" to ―on SL substrate2", the trace resistance does not reduce as significantly, as would be expected since the energy transfer from the laser to the ink is reduced. However, the most interesting result may be that laser scanning on the edge between the SL substrate and ink provides the ―best" reduction in trace resistance. This is most likely a result of improved heating of the ink resulting from both (1) improved absorption of the laser energy in the SL substrate (when compared to the ink), and (2) a combined laser curing approach that uses direct scanning on the ink as well as in-channel heating through the substrate/ink interface. These mechanisms for improved ink curing are the subject of future research. One potential issue with laser scanning, however, is excessive heating of the substrate and/or the ink by the laser. As shown in Figure

3.5(b), there is discoloration on the ink (a brown color) where the laser scanned the ink trace. SEM examination of these ink traces showed no morphological differences for the silver traces between the samples. However, as can be seen in the figure, the laser is charring the SL substrate when the laser scans directly on the substrate. The impact of the laser on the SL substrate is a subject of further research as well as possibly using a reduced laser energy and/or different scanning strategy to eliminate any negative impacts of the laser on both the SL resin and the ink trace. Finally, the data from the repeated laser curing experiment at scan location "on ink" were compared with the first "on ink" results, and showed very similar behavior with an average difference within 8% after the last laser scan pass.

3.4.3 Additional Oven Curing Effect on Trace Resistance

As described in the previous section, *in situ* laser scanning effectively reduces the ink trace resistance so that monolithic structures with integrated electronics can be fabricated in the hybrid SL/DP machine without removal of the part from the machine during fabrication. However, to reduce the time required in the SL machine by minimizing the number of laser scan passes for ink curing, the effects of a post-fabrication thermal cure on trace resistance were explored. If embedded ink traces could be effectively cured using a post-fabrication thermal cure, the number of *in situ* laser scan passes required during fabrication could be minimized. In doing so, the hybrid SL/DP machine is made available for high value production. For this experiment, four test conditions were compared, including two laser scanning conditions (after two and nine laser scanning passes, respectively). Four individual test samples were prepared that consisted of single channels similar to those described in the previous section, but with a channel width of 635 μm (0.025"). The channels were filled with ink and two of the samples were scanned with the laser (two and nine times, respectively), a third sample was left to air dry

for three days in ambient laboratory conditions, and a last sample was designated as the control with no laser scanning or air drying. After laser scanning the first two ink traces, the samples were covered with the ProtoTherm^{TM} 12120 SL resin to embed the traces. After three days, the room temperature air-dried sample was also embedded in the ProtoTherm^{TM} 12120 SL resin. The resin was dispensed using a syringe and cured using a UV light source (Green Spot™, UV Source Inc., American Ultraviolet Company, Lebanon, IN). The last sample designated as a control, was left open and not embedded in resin. The trace resistances on all four samples were recorded before and after oven curing using a Fluke 287 True RMS Multimeter (Fluke Corp., Everett, WA). Although the recommended thermal curing profile for the E-1660 conductive ink is 138°C for 15 minutes, the samples were cured at 80°C for 16 hours due to the limitations of embedded components. The curing was performed in an oven (Imperial V Laboratory Oven, Lab-Line Instrument Inc, Melrose Park, IL), and the time for curing was experimentally determined as sufficiently long to ensure effective trace curing within SL substrates. This 80^{o}C cycle was followed by an additional curing cycle at 120°C for 16 hrs to test if any further reduction in trace resistance could be obtained by increasing the curing temperature closer to the recommended value (138^{o}C) for cases when electronic components capable of higher temperatures are used. Table 3.2 shows the results for these experiments.

Table 3.2. Effect of Oven Curing on Trace Resistance

Channel Width 635 µm (0.025")	Before Oven Curing (Ω)	After Oven Cure at 80°C for 16 Hrs (Ω)	Additional Oven Cure at 120°C for 16 Hrs (After 32 Hrs of Total Oven Curing) (Ω)
Room Temp Air Cured for 3 Days (Embedded)	1.2	0.27	0.29
Laser Cured (9 Passes and Embedded)	0.46	0.31	0.47
Laser Cured (2 Passes and Embedded)	23.2	0.59	0.89
Control (Not Embedded, Not Laser Cured, Not Air Cured)	1.2×10^6	0.17	0.18

The results shown in Table 3.2 indicate that oven curing at 80°C for 16 hours enhances the conductivity (or lowers the measured resistance) of an ink trace regardless of its initial cured state or whether the trace is open to the atmosphere or embedded within an SL resin channel. It does appear, however, that embedding the trace within an SL resin channel may limit the resistance reduction as all embedded trace resistances were greater than the resistance of the open air trace. To determine the statistical significance of these results, additional research is required, but it is important to note that it appears feasible to use a thermal post-cure of a fabricated device to improve trace resistance. It also appears that additional curing even at higher curing temperatures does not improve trace resistance as all samples showed an increase in resistance for further oven curing at 120°C for 16 hrs. Although not a statistical study, the

higher curing temperatures may actually be a source of damage to the trace as a result of possible thermal expansion differences between the ink trace and the substrate, although the details of this interaction is also left for future research. It is sufficient in this case to conclude that oven curing a final fabricated part will benefit the performance of the device.

3.5 Timer Circuit Fabrication Process:

After establishing the SL/DP manufacturing process, the hybrid SL/DP machine was used to demonstrate its capability for fabricating unique and functional 3D structural electronic devices. Similar to previous work (Lopes *et al.*, 2006), the electronic circuit selected for this demonstration was a temperature sensitive, 555-based timer circuit, as depicted in Figure 3.6.

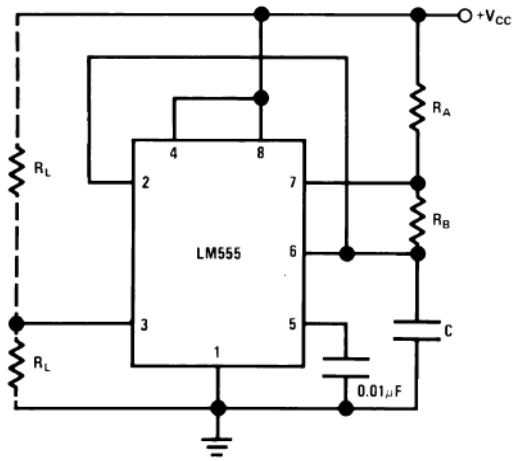

Figure 3.6. The general 555 timer circuit schematic

At the heart of the circuit is a LM555 IC, which includes 23 transistors, 2 diodes and 16 resistors on a silicon chip installed in an 8-pin mini dual-in-line package. In the circuit designed here, the load resistances R_L were replaced by the two LEDs and R_B corresponded to the thermistor resistance. The complete circuit included an external power supply connector (PJ-037A, CUI Inc., Tualatin, OR), a 555 timer chip (LM555, National Semiconductor, Santa Clara, CA), a 2KΩ resistor (291-2K-RC, Arcol/Xicon, Cornwall, UK), a thermistor (2.2 KΩ at 25 °C) (NTCLE100E3222JB0**,** Vishay Intertechnology, Inc., Malvern, PA), a 100 μF capacitor (MAL202134101E3, Vishay Intertechnology, Inc., Malvern, PA), and two LEDs (WP7104YD & WP7104HD, Kingbright Corporation, City of Industry, CA). The simple temperature-sensitive

circuit oscillated the LED at a frequency proportional to the temperature sensed by the thermistor.

3.5.1 2D 555 Timer Fabrication Process

Using the circuit described above, a 2D device was designed first for fabrication using the SL/DP machine (see Figure 3.7). In this example, although the substrate is 3D, all routing was confined to one layer, and as such, this design is considered to be 2D. The part was designed in SolidWorks® with the LM555 timer chip in the center and the remaining components arranged around it, attempting to minimize the size of the overall layout and package as well as minimizing the necessary DP interconnections. The part with the required receptacles, channels, and vias into which the electronic components were press-fitted was built using the SL system. Once the SL part reached a predetermined layer in the build file, the build was interrupted without raising the platform, and the vat was lowered to expose the top surface.

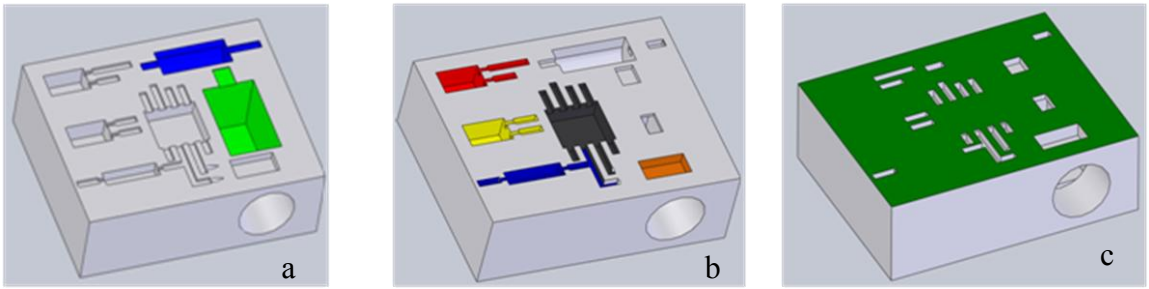

Figure 3.7. Depiction of various SL/DP build stages during the fabrication of the 2D 555 timer circuit: (a) CAD design depicting build stage at which SL build stopped, receptacles and channels cleaned, and power supply socket and capacitor inserted, (b) Build layer at which the remaining electronic components were inserted, (c) Final build layer prior to DP showing access to electronic component pins

The receptacles, channels, and vias were cleaned with Dipropylene Glycol n-Propyl Ether (DPNP) solvent (Univar, Redmond, WA), which was the resin manufacturer‘s recommended solvent for cleaning uncured resin, and commercially available isopropyl alcohol (IPA) to assist in the evaporation of the DPNP solvent after cleaning. A vacuum suction pump (Model No. 400-1901, Barnant Co., Barrington, IL) with ~50 cm (20 inches) Hg suction was subsequently used for removing uncured resin and any remaining cleaning solutions. As mentioned previously, use of the solvent can be avoided if contamination via solvent spillage into the resin vat is a concern, although dimensional inaccuracies may result from unremoved, uncured resin. Figure 3.7(a) depicts the layer at which the build was interrupted, receptacles were cleaned, and the external power supply socket was embedded. The receptacles were designed such that the connector pins of the components were ~100 μm (0.004” or 1 layer thickness) below the last built layer and aligned perpendicular to the SL part surface thus allowing the build to continue with regular Zephyr^{TM} blade sweeping. Figure 3.7(b) shows the layer at which the remaining electronic components were embedded. The resin level was re-adjusted and the build was continued to encapsulate the electronic components while providing access to the corresponding pins in order to complete the interconnections, as depicted in Figure 3.7(c). The SL cleaning process was repeated in preparation for the DP process. The DP nozzle was aligned with the positive pin of the power supply connector and the custom DP script program was initiated to complete the entire DP circuit in one sequence. The part was removed from the SL system, cleaned using DPNP/IPA, cured under a UV light source, and then in a heat convection oven at 80°C and cured for 2 hrs. The maximum operating temperature of the capacitor (85°C) limited the curing temperature to 80°C and since this was below the ink manufacturer‘s recommended curing temperature (138ºC for 15 minutes), two hours of curing was necessary to reach the

manufacturer‘s specified trace resistance as measured during the process. During curing, the resistances of the DP traces were measured using a Keithley 2000 series multimeter (Keithley Instruments Inc., Cleveland, OH).

3.5.2 3D 555 Timer Fabrication Process

To more fully demonstrate the potential of this hybrid manufacturing process, a truly 3D version of the circuit was designed and fabricated. Figure 3.8 represents the process for fabricating the 3D LM 555 timer circuit and illustrates the CAD design depicting the part at various stages during the build. The design shown maintains the same electrical schematic as the previous 2D version, but now includes components at different depths within the substrate and vias between layers to demonstrate the freedom in component placement and routing brought to bear by this hybrid fabrication technology. Otherwise, the process used for this device is identical to the 2D process, but involved additional repetitions as shown in the flow chart in Figure 3.4. The 3D design also incorporates channels for housing the conductive traces and assisting in vertical vias alignment during the fabrication process. Figure 3.8(a) depicts the first SL build stop, where receptacles were cleaned and the first electronic components were embedded. Figure 3.8(b) illustrates the build stage at which the first DP process and laser ink curing was carried out. A separate _.stl‘ file was used to cure the ink using the SL laser at 97.7 mW laser power at a depth of penetration value (D_P) of 1.25, which corresponds to a laser speed of ~480 μm/s. The ink curing process consisted of tracing the laser across the DP interconnects five times as determined in our previously described experiments to ensure satisfactory ink curing as measured using a standard Keithley series 2000 multimeter. This cure required 30 minutes to complete (recall from Figure 3.5(c) that five laser passes ensured in every case that the solvent evaporation phase was complete and the ink binder curing process was proceeding).

Figure 3.8(c) shows the second SL build stop, where the receptacles were cleaned and the second set of components were embedded. Figure 3.8(d) depicts the build stage at which the second DP process and laser ink curing were implemented. The two separated DP layers were connected using the vertical vias, which were manually filled with ink. The complete part was cleaned, cured in an UV oven, and then in a temperature oven at 80°C for 16 hours. The oven curing duration was extended to 16 hours to help ensure a minimum trace resistance for the inked vias, due to the temperature limitation imposed by the operating temperature of the capacitor (85°C).

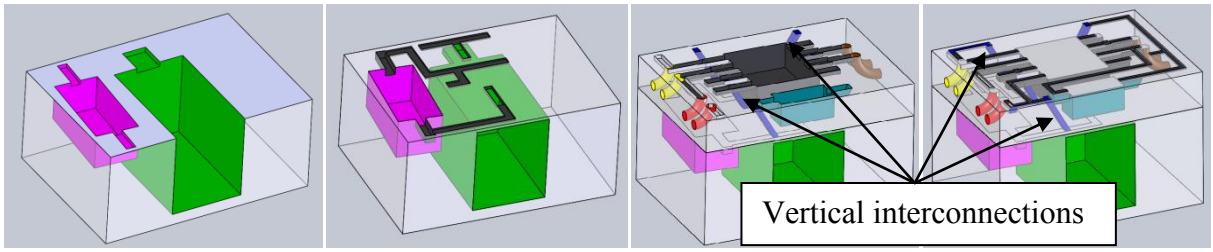

(a) (b) (c) (d)

Figure 3.8. CAD design depicting the build stages during 3D 555 timer circuit fabrication: (a) First SL build stop, receptacles cleaned, and first set of electronic components inserted, (b) Continue SL to embed components and build channels, second SL build stop, channels cleaned, first DP process and laser ink curing, (c) Continue SL build, third SL build stop, receptacles and channels cleaned, and second set of components inserted (d) Second DP process and laser ink curing

Some of the key process features necessary for truly 3D designs fabricated in the hybrid SL/DP technology were:

- Design freedom to select an optimum arrangement of component receptacles, interconnect channels and vias in the circuit using CAD – in order to minimize size and potentially

conform to application requirements such as human anatomy or mechanical volume requirements,

- Channels for delineating the conductive ink traces, maintaining large aspect ratios in order to reduce overall resistance, while simultaneously providing dense routing with minimum trace pitch, providing a wide range of trace widths, and assisting in vertical vias alignment during the 3D fabrication process,
- In-process cleaning of receptacles and vias using recommended cleaning solutions and a vacuum-assisted removal process,
- Accurate on-demand dispensing of conductive ink and virtually any material (i.e. very wide range of materials in terms of viscosity), and
- Curing with the SL laser the conductive ink traces providing a continuous 3D manufacturing capability.

3.6 Demonstration of the 555 Timer Circuit:

The 2D and 3D 555 timer circuits were successfully fabricated using the fabrication process. The duty cycle and frequency of the blinking LEDs in the circuits were measured using the Fluke PM3380B 100 MHz Combiscope (Fluke Corp., Everett, WA) and compared with the expected theoretical values. The equations for expected frequency and duty cycle (LM555.pdf, National Semiconductor, Santa Clara, CA) were as follows, although these equations do not account for the resistances in the interconnects, which for traditional PCB technologies is less than 1 ohm. For designs using printed conductors with generally higher parasitic resistance values, an error term would be introduced to both resistance values.

$$Frequency\ (F) = \frac{1.4}{(R1\ +\ 2\ *\ R2)\ *\ C1}$$

$$Duty\ Cycle\ (D) = \frac{(R1\ +\ R2)}{(R1 + 2\ *\ R2)}$$

Where, R1 = Resistance of resistor

R2 = Resistance of thermistor at room temperature

C1 = Capacitor rating in F

3.6.1 2D LM 555 Timer Circuit

Figure 3.9 shows the actual SL part during the various stages of the SL/DP build procedure used to manufacture the 2D LM 555 timer circuit. Figure 3.9(a) shows the build stage at which the electronic components were embedded. Figure 3.9(b) shows the DP interconnections between the various electronic components. The total time for manufacturing

the completed part with embedded components and DP interconnections was approximately three and a half hours, which included 2 hrs of thermal post-cure. The process required two SL interruptions, ~15 minutes to place the components, ~10 minutes for cleaning and uncured resin removal, ~20 minutes for SL/DP registration and inking, ~15 minutes for final cleaning, 30 minutes of UV post-curing, and 2 hrs for post-curing at 80°C in an oven.

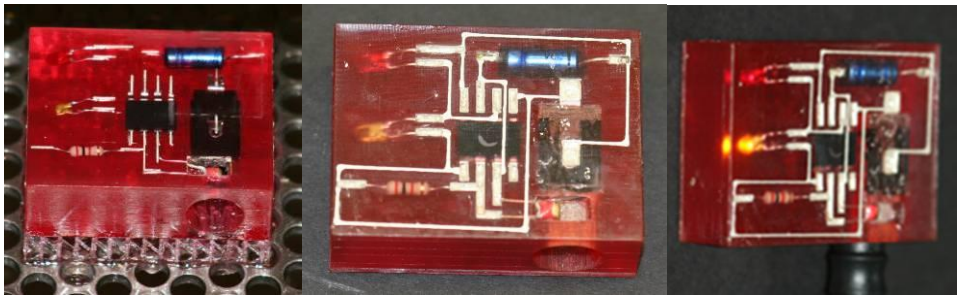

(a) (b) (c)

Figure 3.9. Fabrication of 2D555 timer circuit: (a) SL part with embedded components and DP interconnections, (b) SL part with DP interconnects, (c) Final working circuit (note the activated yellow LED)

The circuit worked and responded to temperature changes as depicted by the frequency of the blinking LEDs (see activated LED in Figure 3.9(c)). The measured frequency and duty cycle of the 2D 555 timer circuit at room temperature were 2.19 Hz and 67 %, respectively. The corresponding theoretical values of frequency and duty cycle for the 2D 555 timer circuit was 2.25 Hz and 65.7 %, respectively, or the measured values were within 5 % of the theoretical values and this error can be accounted for by the increased resistivity of the conductive inks relative to the ideal circuit.

3.6.2 3D LM 555 Timer Circuit

The fabrication process tailored for 3D electronics was utilized to manufacture the 3D LM 555 timer circuit. Figure 3.10 shows the actual 3D555 timer circuit with embedded

electronics. The circuit operated as expected - responding to temperature changes by changing the frequency of the blinking LEDs. The measured frequency and duty cycle of the 3D 555 timer circuit at room temperature was 2.5 Hz and 67 %, respectively (recall the theoretical values of 2.25 Hz and 65.7%, respectively, as described previously). The variation of 5% for the duty cycle was within the standard tolerances of the resistor and thermistor components. The 10% variation in the frequency measurements can be attributed to the parasitic resistances arising from the 3D vias. The total time for manufacturing the completed part was approximately 2 hours and required an additional 16 hrs of thermal post curing. The process required three SL interruptions, ~15 minutes to place the components, ~10 minutes for cleaning and uncured resin removal, ~20 minutes for SL/DP registration and inking, ~30 minutes for *in situ* laser curing, ~15 minutes for final cleaning, 30 minutes of UV post-curing, and an additional 16 hrs for post-curing at 80°C in an oven.

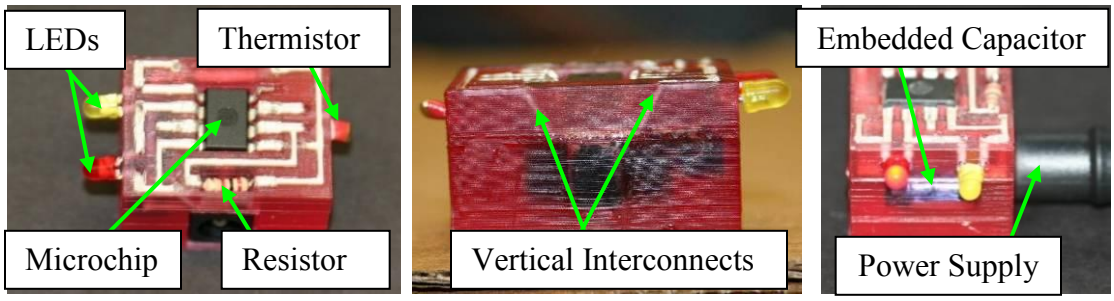

(a) **(b)** **(c)**

Figure 3.10. Fabrication of the 3D 555 timer circuit: (a) 3D 555 timer circuit, (b) vertical interconnects, (c) working 3D circuit (note the activated yellow LED)

3.7 Discussion:

This work broadly demonstrates what can be achieved by integrating multiple AM technologies together for fabricating unique devices and more specifically demonstrates a hybrid SL/DP machine that can fabricate unique, monolithic 3D embedded electronic circuits. Although the demonstrated circuit was a low power application (< 0.5 Watts), the processes and technology described here can be applied to high powered circuits by, for example, incorporating novel active and passive cooling strategies in the design (i.e., embedding a heat pipe in the SL substrate). Beyond power requirements, the 555 timer circuit used in this evaluation requires only a single layer of routing and does not represent the complication of more sophisticated electronics requiring multi-layered routing. Furthermore, the electrical performance requirements in terms of operating frequency were also low and not representative of most modern electronics. Figure 3.11 shows two applications in which structural electronics were fabricated with RF antennas, dense routing and on conformal and 3D surfaces. Although these applications were not fabricated within the hybrid SL/DP machine described in this paper within a single build, future research on this system will make this possible through improved process planning and automation of many of the processes and procedures described in this paper. In the examples in Figure 3.11, the interconnect for these two devices was printed manually due to interconnect complexity, but these devices still serve to illustrate the potential for compelling structural electronic applications in bio-medical, commercial and defense electronics. The left example is a magnetometer in which hall-effect sensors are placed orthogonally to a microprocessor. The right example is a conformal helmet insert with an accelerometer required to detect traumatic head injury.

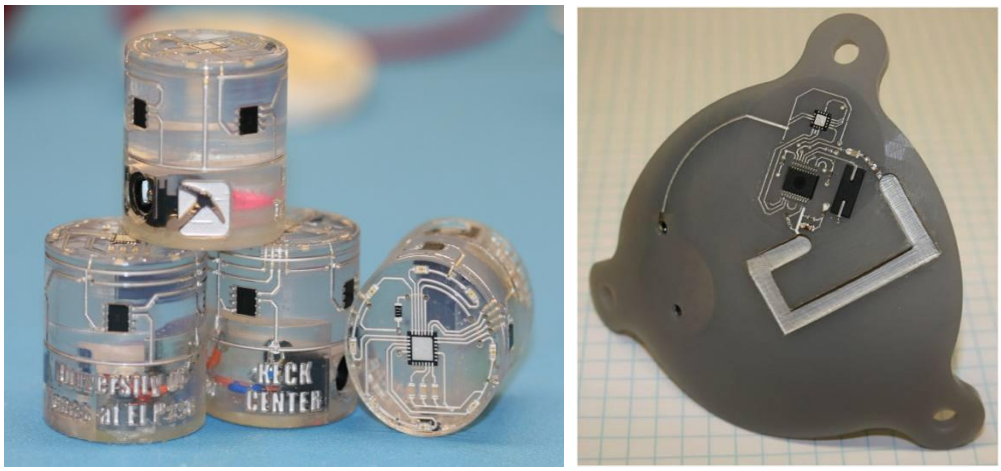

Figure 3.11. Examples of 3D Structural Electronics

3.8 Conclusions and Future Work:

This paper presents a hybrid manufacturing system that integrates SL and DP technologies to fabricate 3D structures with embedded electronic circuits. A functional SL/DP manufacturing process was developed to fabricate 2D and 3D monolithic structures with embedded electronics and circuitry. The process involved part design, process planning, integrated manufacturing including multiple starts and stops of both SL and DP, and post-processing. The integrated 3D micro-dispensing system provided control over DP dispensing and combined with the manufacturing flexibility of the SL machine enabled the fabrication of a 3D electronic device within the hybrid SL/DP machine. To enable fabrication of 3D electronic circuits without removal of the part from the SL/DP machine during fabrication, an *in situ* laser scanning procedure using the SL laser was developed that sufficiently cured the conductive ink traces in the machine so that the SL build could continue. Although the process does not require removal of the structure from the machine during fabrication, many of the current sub-processes are manual. As a result, further development is required for complete automation of the manufacturing process. Advanced applications are demonstrated using a semi-automated approach to SL/DP integration.

Opportunities exist to fully automate the hybrid SL/DP machine and process for enhancing the commercial appeal for fabricating complex systems. Laser scanning of surface contours and 3D linear positioning systems are techniques that can enable automated SL/DP registration and help optimize the fabrication process. Improved vertical via design, automated cleaning, and optimized laser curing can help achieve improved multilayer trace conductivity. Achieving full automation of the SL/DP process and optimizing the vertical interconnects are important areas of future research that will enable critical advancement in this technology.

Incorporating surface mount components can further assist in the miniaturization of the final circuit.

3.9 Acknowledgements:

The research presented here was performed at the University of Texas at El Paso (UTEP) within the W.M. Keck Center for 3D Innovation (Keck Center). Many past and current students, staff, and faculty associated with the Keck Center contributed in various ways to the development and use of the hybrid stereolithography and direct print machine, and all contributions to the advancement of this technology are appreciated. In particular, the authors would like to thank Dan Muse, Richard Olivas, Rodolfo Salas, Mohammed Alawneh, Misael Navarrete, David Roberson, Frank Medina, Dr. In Hwan Lee, and Dr. Karina Arcaute for their assistance on various aspects of the research. The research described here was based, in part, upon work supported through research contract N000140710633 from the Office of Naval Research, research Contract No. W9113-08-C-0010 from the U.S. Army Space and Missile Defense Command and the Homeland Protection Institute to the UTEP Center for Defense Systems Research, research contract 504004 from Sandia National Laboratories, and the endowed Mr. and Mrs. MacIntosh Murchison Chair I in Engineering at UTEP. Sandia National Laboratories is a multi-program laboratory operated by Sandia Corporation, a Lockheed Martin Company, for the United States Department of Energy's National Nuclear Security Administration under contract DE-AC04-94AL85000. The findings and opinions presented here are those of the authors and do not necessarily reflect those of the sponsors of this research.

3.10 References:

Arnold, C., Serra, P. and Piqué, A. (2007), "Laser direct-write techniques for printing of complex materials", *MRS Bulletin,* Vol. 20, pp. 29-36.

Banfield, D. (2000), "Understanding and measuring electrical resistivity in conductive inks and adhesives", *SGIA Journal*.

Bieri, N., Chung, J., Haferl, E., Poulikakos, D. and Grigoropoulos, C. (2003), "Microstructuring by printing and laser curing of nanoparticle solutions", *Applied Physics Letters*, Vol. 82 No. 20, pp. 3259-3531.

Castillo S., Muse D., Medina F., MacDonald E. and Wicker R. (2009), "Electronics integration in conformal substrates fabricated with additive layered manufacturing", *Proceedings of the 20th Annual Solid Freeform Fabrication Symposium*, University of Texas at Austin, Austin, TX, pp. 730-737.

Cham, J., Pruitt, B., Cutkosky, M., Binnard, M., Weiss, L. and Neplotnik, G. (1999), "Layered manufacturing with embedded components: process planning considerations", *Proceedings of DETC99: 1999 ASME Design Engineering Technical Conference*, September 12-15, Las Vegas, NV.

Chartier, T., Duterte, C., Delhote, N., Baillargeat, D., Verdeyme, S., Delage, C. and Chaput, C. (2008), "Fabrication of millimeter wave cmponents via ceramic stereo- and microstereolithography processes", *Journal of the American Ceramic Society*, pp. 2469-2479.

Chrisey, D.B. and Pique, A. (2002), *Direct-Write Technologies for Rapid Prototyping Applications: Sensors, Electronics, and Integrated Power Sources*, Harcourt Inc.: Academic Press, San Diego, California.

Church, K.H., Fore, C. and Feeley, T. (2000), "Commercial applications and review for direct write technologies", *Materials Development for Direct Write Technologies,* San Francisco, CA, April 24-26, Vol. 624, pp. 3-8.

Czajkiewicz Z. (2008), "Direct digital manufacturing - new product development and production technology", *Economics and Organization of Enterprise*, Vol. 2, pp. 26-37.

De Laurentis, K., Mavroidis, C. and Kong, F. (2004), "Fabrication of non-assembly robotic systems with embedded components using rapid prototyping system", *IEEE Robotics and Automation Magazine*, pp. 86-92.

De Nava, E., Muse, D., Castillo, S., Alawneh, M., Navarrete, M., Lopes, A.J., MacDonald, E. and Wicker, R.B. (2008), "3D off-axis component placement and routing with solid freeform fabrication", *Proceedings from the 19th Annual Solid Freeform Fabrication Symposium*, University of Texas at Austin, August 3-5, pp. 362-369.

Doreau, F. Chaput, C. and Chartier, T. (2000), "Stereolithography for manufacturing ceramic parts", *Advanced Engineering Materials*, pp. 493-496.

Fearon, E., Sato, T., Wellburn, D., Watkins, K. and Dearden, G. (2007), "Thermal effects of substrate materials used in the laser curing of particulate silver inks", *Laser Assisted Net Shaping Engineering 5, Proceedings of the LANE*, pp. 379-390.

Greer, J.R. and Street, R.A. (2007), "Thermal cure effects on electrical performance of nanoparticle silver inks", *Acta Materialia,* Vol. 55, pp. 6345–6349.

Hecht, E. (2002), *Optics, 4th Edition*, Published by Addison and Wesley, San Francisco, CA, ISBN 0-8053-8566-5.

Inamdar A., Magana M., Medina F., Grajeda Y. and Wicker R. (2006), "Development of an automated multiple material stereolithography machine", *Proceedings of the 17th Annual*

Solid Freeform Fabrication Symposium, University of Texas at Austin, Austin, TX, pp. 624-635.

Jacobs, P.F. (1992), *Rapid prototyping & Manufacturing: Fundamentals of stereolithography*, Published by Society of Manufacturing Engineers, Dearborn, Michigan.

Jagt, J. (1998), "Reliability of electrically conductive adhesive joints for surface mount applications: A Summary of the State of the Art", *IEEE Transactions on Components, Packaging, and Manufacturing Technology—Part A*, Vol. 21 No. 2, pp. 215-225.

Janaki Ram, G.D., Robinson C., Yang Y. and Stucker, B.E. (2007), "Use of ultrasonic consolidation for fabrication of multi-material structures", *Rapid Prototyping Journal*, Vol. 13 No. 4, pp. 226–235.

Kataria, A. and Rosen, D.W. (2001), "Building around inserts: methods for fabricating complex devices in stereolithography", *Rapid Prototyping Journal,* Vol. 7 No. 5, pp. 253-261.

Kim, D. and Moon, J. (2005), "Highly conductive inkjet printed films of nanosilver particles for printable electronics", *Electrochemical and Solid State Lasers*, Vol. 8 No. 11, pp. 130-133.

Kruth, J.P., Leu, M.C. and Nakagawa, T. (1998), "Progress in additive manufacturing and rapid prototyping", *CIRP Annals - Manufacturing Technology*, Vol. 47 No. 2, pp. 525-540.

Longtin, J., Sampath, S., Tankiewicz, S., Gambino, R. and Greenlaw, R. J. (2004), "Sensors for harsh environments by direct-write thermal spray", *IEEE Sensors Journal,* Vol. 4 No. 1, pp. 118-121.

Lopes, A.J., Navarrete, M., Medina, F., Palmer, J., MacDonald, E. and Wicker, R.B. (2006), "Expanding rapid prototyping for electronic systems integration of arbitrary form", *Proceedings of the 17th Annual Solid Freeform Fabrication Symposium*, University of Texas at Austin, Austin, TX.

Malone, E. and Lipson, H. (2006), "Freeform fabrication of ionomeric polymer-metal composite actuator", *Rapid Prototyping Journal*, Vol. 12 No. 5, pp. 244-253.

Malone, E., Berry, M. and Lipson, H. (2007), "Freeform fabrication and characterization of zn-air batteries", *Rapid Prototyping Journal*, Vol. 14 No. 3, pp. 128-140.

Medina, F., Lopes, A.J., Inamdar, A.V., Hennessey, R., Palmer, J.A., Chavez, B.D. and Wicker, R.B. (2005a), "Integrating multiple rapid manufacturing technologies for developing advanced customized functional devices", *Rapid Prototyping & Manufacturing 2005 Conference Proceedings,* Rapid Prototyping Association of the Society of Manufacturing Engineers, Hyatt Regency Dearborn, Michigan, 2005a.

Medina, F., Lopes, A.J., Inamdar, A., Hennessey, R., Palmer, J., Chavez, B., Davis, D., Gallegos, P. and Wicker, R.B. (2005b), "Hybrid manufacturing: integrating stereolithography and direct write technologies", *Proceedings of the 16th Annual Solid Freeform Fabrication Symposium*, University of Texas at Austin, Austin, TX, pp. 39-49.

Merilampi, S., Laine-Ma, T. and Ruuskanen, P. (2009), "The characterization of electrically conductive silver ink patterns on flexible substrates", *Microelectronics Reliability*, Vol. 49, pp. 782 – 790.

Mo, L., Liu, D., Zhou, X. and Li, L. (2009), "Preparation and conductive mechanism of the ink-jet printed nanosilver films for flexible display", *2nd International Congress on Image and Signal Processing*, ISBN # 978-1-4244-4129-7.

Mosses, R. and Brackenridge, S. (2003), "A novel process for the manufacturing of advanced interconnects", *Circuit World*, Vol. 29 No. 3, pp. 18-21.

Navarrete M., Lopes A., Acuna J., Estrada R., MacDonald E., Palmer J. and Wicker R. (2007), "Integrated layered manufacturing of a novel wireless motion sensor system with GPS",

Proceedings of the 18th Annual Solid Freeform Fabrication Symposium, University of Texas at Austin, August 6-8, pp. 575-585.

Palmer, J.A., Yang, P., Davis, D.W., Chavez, B.D., Gallegos, P.L., Wicker, R.B. and Medina, F.R. (2004), "Rapid prototyping of high density circuitry", *Rapid Prototyping & Manufacturing 2004 Conference Proceedings*, Rapid Prototyping Association of the Society of Manufacturing Engineers, Hyatt Regency Dearborn, Michigan. Also, *SME Technical Paper TP04PUB221* (Dearborn, Michigan: Society of Manufacturing Engineers).

Palmer, J.A., Summers, J.L., Davis, D.W., Gallegos, P.L., Chavez, B.D., Yang, P., Medina, F. and Wicker, R.B. (2005), "Realizing 3-D interconnected direct write electronics within smart stereolithography structures", *International Mechanical Engineering Congress and Exposition 2005 Proceedings*, November 14-18, Orlando, Florida.

Park, B. K., Kim, D., Jeong, S., Moon J. and Kim, J. S. (2007), "Direct writing of copper conductive patterns by ink-jet printing", *Thin Solid Films*, Vol. 515, pp. 7706–7711.

Periard, D., Malone, E. and Lipson, H. (2007), "Printing embedded circuits", *Proceedings of the 18th Solid Freeform Fabrication Symposium*, Austin TX, pp. 503-512.

Pique, A., Mathews, S.A., Pratap, B., Auyeung, R.C.Y., Karns, B.J. and Lakeou, S. (2006), "Embedding electronic circuits by laser direct-write", *Microelectronic Engineering*, Vol. 83, pp. 2527-2533.

Pudas, M., Halonen, N., Granat, P. and Vahakangas, J. (2005), "Gravure printing of conductive particulate polymer inks on flexible substrates", *Progress in Organic Coatings 54*, pp. 310–316.

Robinson C.J., Stucker B., Lopes A.J., Wicker R.B. and Palmer J.A., (2006), "Integration of direct-write (DW) and ultrasonic consolidation (UC) technologies to create advanced structures with embedded electrical circuitry", *Proceedings of the 17th Annual Solid Freeform Fabrication Symposium*, University of Texas at Austin, Austin, TX, pp. 60-69.

Tuck, C. and Hague, R. (2007), "Rapid manufacturing: impact on supply chain methodologies and practice", *International Journal of Services and Operations Management*, Vol. 3 No. 1, pp. 1-22.

Young, D., Sampath, S., Chikov, B. and Chrisey, D.B. (2005), "The future of direct writing in electronics", *CircuiTree.*

Weiss, L.E., Merz, R., Prinz, F.B., Neplotnik, G., Padmanabhan, P., Schultz, L. and Ramaswami, K. (1997), "Shape deposition manufacturing of heterogeneous structures", *SME Journal of Manufacturing Systems*, Vol. 16 No. 4, pp. 239-248.

Weiss, L. and Prinz, F. (1998), "Novel applications and implementations of shape deposition manufacturing", *Naval Research Reviews, Office of Naval Research, Three*, Vol. L.

Wohler's Report (2010), Wohler's Associates, Fort Collins, CO, ISBN 0-9754429-6-1.

DARPA DSO (2010), http://www.darpa.mil/dso/archives/mice/ (accessed 28 May 2010).

DSM Somos ProtoTherm™ 12120 –Product Data Sheet, DSM Somos, New Castle: Delaware, www.dsmsomos.com, accessed on 03/27/2005.

E-1660 Product Data Sheet, www.erconinc.com*, (accessed on 15 May 2010).*

nScrypt Inc., http://www.nscryptinc.com/smartpump/ , (accessed 9 June 2010).

Thermometrics Inc., http://www.gesensing.com/products/resources/whitepapers/ntcnotes.pdf (accessed on 10 May 2010).

Chapter 4

LASER CURING OF SILVER-BASED CONDUCTIVE INKS FOR 3D STRUCTURAL ELECTRONICS IN STEREOLITHOGRAPHY

The material of this chapter is taken from the journal paper titled ‗Laser Curing of Silver-Based Conductive Inks for 3D Structural Electronics in Stereolithography' that will be submitted to the Journal of Materials Processing Technology, and will be a copyright of Elsevier. The author would like to thank the Journal of Materials Processing Technology and Elsevier for giving advance permission to include this material as part of my dissertation.

4 LASER CURING OF SILVER-BASED CONDUCTIVE INKS FOR 3D STRUCTURAL ELECTRONICS IN STEREOLITHOGRAPHY

Amit J. Lopes[1], In Hwan Lee[2], Eric MacDonald[1], Rolando Quintana[3], Kenneth Church[1,4], and Ryan Wicker[1]

[1]W.M. Keck Center for 3D Innovation, The University of Texas at El Paso, El Paso, Texas, USA

[2]School of Mechanical Engineering, Chungbuk National University, Cheongju, Korea

[3]Department of Management Science and Statistics, The University of Texas at San Antonio, San Antonio, Texas USA

[4] nScyrpt, Inc., Orlando, Florida

Abstract

A hybrid Stereolithography (SL) / Direct Print (DP) system has been developed to fabricate three-dimensional (3D) structural electronic devices in which component placement, interconnect routing, and systems boundaries are not confined to two dimensions as is the case with traditional Printed Circuit Boards (PCBs). The resulting increased level of design and fabrication freedom provides potential for a reduction in both volume and weight as well as the capability of these systems to be fabricated in arbitrary and complex shapes as required to conform to unique application requirements (e.g. human anatomy, airframe structures, and other volumetrically-constrained mechanical systems). The fabrication of these devices without intermediate part removal between SL and DP processes as described previously requires in situ Ultra Violet (UV) laser curing of silver-based inks to sufficiently cure the inks prior to continuing additional SL fabrication. This paper describes investigations into improvements of the laser curing process. The hybrid SL / DP system comprised of both a 3D Systems SL 250/50 machine and an nScrypt micro-dispensing pump was used to fabricate samples for the laser

curing experiments. Various laser curing parameters, including energy (laser power and scan speed), scanning location and laser wavelength were investigated. The trace resistances and structural changes in SL substrate and printed conductive ink for each experiment were compared to determine the best laser ink curing method. Preliminary experiments on the effect of laser curing of a variety of conductive inks included using a standard solid-state SL laser (355 nm) with a power level of ~95 mW and a scan speed of ~480 µm/s. Scanning on the substrate adjacent to the ink channel resulted in the most effective ink curing but resulted in charring of the substrate. Comparatively, when laser power was reduced sufficiently to eliminate the charring, relatively lower effective ink curing was achieved. Alternatively, laser curing of conductive ink at 325 nm wavelengths (used in older generation stereolithography systems) was relatively more effective due to higher energy absorption by the silver particles at that wavelength. Furthermore, oven curing of partially laser cured ink traces was investigated to determine the minimum number of in situ laser passes required during SL fabrication. Results indicated that particulate silver based conductive inks can be successfully cured in situ using a SL UV laser with various laser curing parameters.

Keywords: *In situ UV laser curing, 3D structural electronics, Direct print, Multiple materials*

4.1 Introduction:

Electronics require continual advancements in fabrication technology to provide smaller, lighter, more efficient and faster devices. Traditionally, electronics consist of a Printed Circuit Board (PCB) made up of electronic components interconnected with conductive traces patterned onto a non-conductive substrate. However, a substantial reduction in circuit volume and weight can be realized by embedding electronic components within truly 3D dielectric substrates at various depths and orientations. Recently, several researchers have explored the capabilities of using traditional Additive Manufacturing (AM) or Rapid Prototyping (RP) technology in the context of fabricating and prototyping functional products including conformal three-dimensional (3D) structural electronic devices (Lopes *et al.*, 2010). This research is a continued development of the work done by Lopes *et al.*, 2006 where stereolithography (SL) and DP were combined in a single hybrid manufacturing system for developing unique structural electronics packages. A structural component was fabricated using SL and DP used to complete the required interconnections between the embedded electronic components, without the need for intermediate part removal.

Several researchers have combined AM and Direct Print (DP) systems for fabricating complex electronics systems. Weiss and Prinz (1998) utilized the shape deposition manufacturing technology to manufacture a novel waterproof wearable computer with embedded electronics. Church *et al.* (2000) created wireless sensor systems using an advanced DP system to print conductive lines onto glass substrates. Pique *et al.* (2006) demonstrated the use of a laser direct write process for embedding electronic circuits in two dimensions within flexible substrates. Robinson *et al.* (2006) manufactured electronic circuitry, antennae and other devices directly into a solid metal structure fabricated in Ultrasonic Consolidation (UC) by integrating

DP ink dispensing and UC. Malone and Lipson (2006) utilized the Fab@Home AM machine and developed novel material formulations to fabricate ionomeric polymer-metal composite actuators. As a continued advancement of structural electronics fabrication, a hybrid SL/DP system and process was utilized to develop complex freeform packages with embedded 3D Structural Electronics (Lopes *et al.*, 2010).

For realizing functional interconnects using DP, a wide range of metals namely gold, silver, copper, and nickel can be utilized (Jagt, 1998). Development of nanoparticle ink has advanced the inkjet printing of copper and silver nanoparticles and advanced the capabilities of DP (Mo *et al.,* 2009; Park *et al.,* 2007). Thermally curing of nanoparticle inks results in a sintered microstructure at temperatures (>150°C for 30 minutes) well below the melting temperature of the bulk metal due to the beneficial scaling effect on the melting point of the particles (Kim and Moon, 2005; Greer and Street, 2005). Micro-particle inks are generally more viscous than nanoparticle inks and conduct well without sintering or melting due to the percolation effect, which results in a binder/silver particle composite matrix (Saraf *et al.*, 1995). The resulting ink curing process leads to a network of interconnected conductive particles facilitated by the relatively high contact area between the particles (Pudas *et. al.,* 2005). For this research, flake-based silver inks were investigated as part of the *in situ* UV laser curing experiment. The experiments were restricted to SL parts fabricated in a commercial SLA 250/50 machine using traditional SL lasers. Furthermore, the results were compared with similar curing of nanoparticle silver ink and relatively more viscous micro-particle silver inks to examine whether the above laser curing results are ink–specific or can be generalized.

Although most conductive inks are thermally cured in temperature-controlled ovens, several researchers have utilized a variety of lasers as an alternative method for selective curing

of a variety of conductive media (Bieri *et al.*, 2003; Chung *et al.*, 2004; Palmer *et al.*, 2005; Ko *et al.*, 2006; Fearon *et al.*, 2007) . The laser curing process is: 1) much faster than traditional oven curing for curing with short scan lengths, 2) capable of localized curing while protecting nearby heat sensitive electronic components and substrates, and 3) an enabler of the fabrication of 3D structural electronic devices by providing sufficient curing of the conductive traces *in situ* during the manufacturing process and thus allowing for fabrication of subsequent AM layers without ink/resin contamination (Fearon *et al.*, 2007). The third aspect allows for the continual fabrication of structural electronics without requiring removal of the partially-built structures. Bieri *et al.* (2003) utilized an argon-ion laser at 488 nm wavelength to cure a conductive ink comprised of 30% gold nanoparticle in a toluene solution with a goal of manufacturing microstructures from metal nanoparticles. The optical behavior of the nanoparticle solution impacted the selection of the wavelength of the laser. The solvent evaporates as a result of the laser radiation, which is absorbed in the gold nanoparticles and results in thermal diffusion towards the evaporation interfaces (Chung *et al.*, 2004). Palmer *et al.* (2005) utilized an 800nm femtosecond laser to cure silver based ink as part of the process for fabricating a functional power supply voltage converter circuit capable of electromagnetic interference filtering. Ko *et al.* (2006) demonstrated the utilization of a frequency doubled neodymnium doped yttrium aluminum garnet nanosecond laser having pulse width between 3–5 ns to sinter an alkanethiol self-assembled monolayer protected gold nanoparticle film on polyimide substrate. Fearon *et al.* (2007) demonstrated the utilization of an 8.1 W CO_2 laser to cure flake based conductive ink consisting of particulate silver, a resin binder, and solvents added for lowering the viscosity. The ink was cured by laser energy absorption by the silver particles and resin binder and the resulting heat buildup evaporates the solvent and cures the resin binder leading to a continuous network of

interconnected silver particulates. Maekawa *et al.* (2009) examined the effect of a range of wavelengths (488nm – 1064 nm), using a variety of laser sources, on laser sintering characteristics of Ag nanoparticles as well as adhesion of the cured ink to a polyimide substrate.

These developments illustrated the feasibility of utilizing lasers to effectively cure a variety of conductive inks. However, there is limited research on *in situ* UV laser curing of conductive inks as part of 3D Structural Electronics fabrication. Consequently, this research demonstrates the utilization of standard 355 nm and 325 nm SL lasers, which can facilitate integrated SL part building and *in situ* conductive ink curing to fabricate 3D structural electronic devices. As mentioned earlier, there are several methods to fabricate 3D structural electronics devices. However, *in situ* laser curing is essential when fabricating monolithic 3D structural electronic devices in an integrated hybrid AM/DP system without requiring intermediate part removal. As a result, this research investigates *in situ* UV laser curing of conductive inks within a stereolithography system to help determine the conditions for an effective and efficient laser curing process with the goals: 1) to sufficiently cure the inks to allow for continued fabrication with a resin based process and 2) to improve (or decrease) interconnect resistance, and 3) to reduce manufacturing time during the 3D structural electronic device fabrication process. In an SL system, each resin has a recommended critical exposure (E_c) and depth of penetration (D_p) parameter required to build each layer of the SL part. The speed at which the laser traverses for building the SL part is determined through the SL control software by the laser power and D_p for a given E_c. This control feature of an SL system is used to control the supplied laser energy for the *in situ* ink curing experiments. As part of this research, several laser parameters including laser energy (based on laser power and scan speed), scanning location relative to the ink to be cured, and laser wavelength were analyzed. Additionally, the effects of a post-fabrication

thermal cure on trace resistance were explored to determine the minimum number of laser scanning passes (and thus, minimum time required) for ink curing in the context of a final full oven cure after the fabrication. Finally, laser curing experiments were performed using a variety of inks to determine if a specific type of ink was more responsive to curing by laser as well as to determine if the results could be generalized.

4.2 Systems and Materials:

4.2.1 SL/DP System

A hybrid SL/DP system developed by Lopes *et al.* (2010) was utilized to fabricate the test samples required for the experiments. Figure 4.1 represents a schematic of the hybrid SL/DP system that illustrates a simple integration of the separate SL and DP systems. The basic configuration of the hybrid system has been described in several previous publications (Lopes *et al.*, 2006; Navarrete *et al.*, (2007); DeNava *et al.*, (2008); Castillo *et. al.* (2009); Lopes *et al.*, 2010). Specifically, a commercial 3D Systems 250/50 SL machine (3D Systems, Rock Hill, SC) equipped with a 355 nm solid-state laser upgrade (Series 3500-SMPS, DPSS Lasers Inc., Santa Clara, CA) was selected as the SL system. An advanced nScrypt Smart Pump™ 100 (nScrypt, Inc, Orlando, FL) was selected as the micro-dispensing tool due to its ability to dispense very small volumes of material (10^5 μm^3) over a wide range of viscosities (0.001 Pa-s to 1,000 Pa-s).

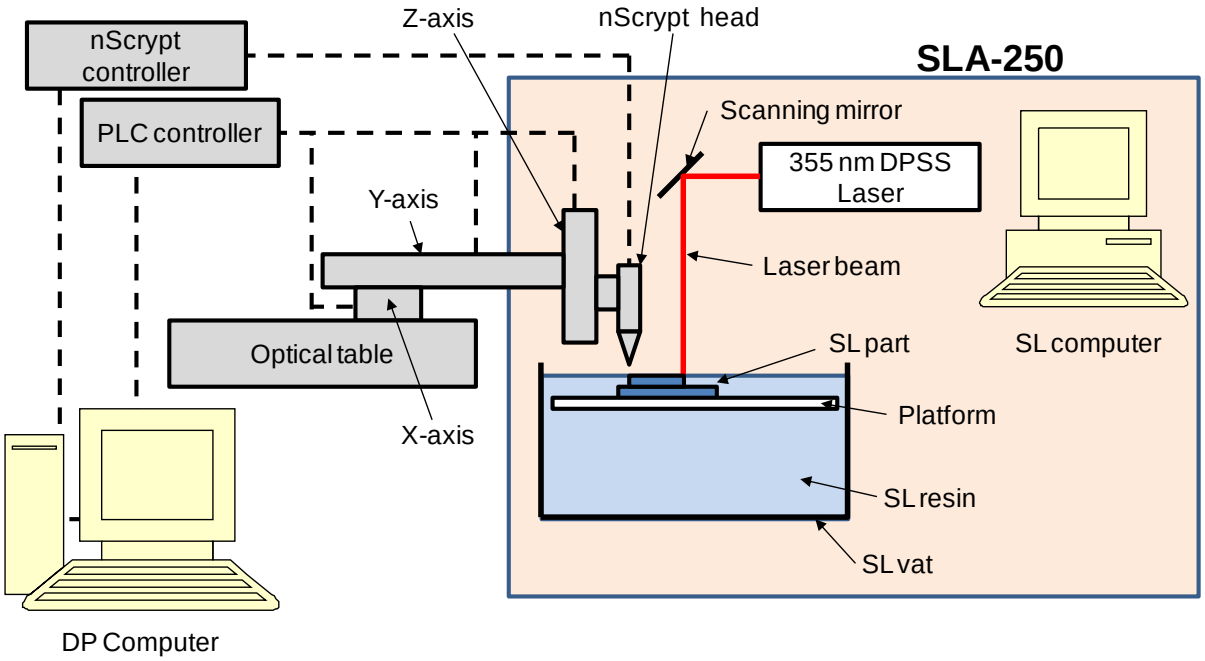

Figure 4.1. Schematic of the hybrid SL/DP system

The DP pump was attached to the z-stage of the orthogonally-aligned precision 3-axis linear positioning stages (Parker Hannifin Corporation, Electromechanical Automation Division, Rohnert Park, CA). The entire DP setup was placed on a custom optical table (Custom VH3660W IsoStation, Model # 04SI69128, Newport Corporation, Mountain View, CA), which was aligned with the SL system. The 3 axis traverse system was controlled using an integrated programmable logic controller and the nScrypt controller managed the DP dispensing process. A custom DP control program written in an assembly language script was used to interface between the control software of the stages and the nScrypt dispensing system.

4.2.2 Materials

The materials used for conductors and dielectrics are described in greater detail in Lopes *et al.*, 2010. Specifically, the ProtoTherm^{TM} 12120 (DSM Somos®, Elgin, IL) resin was selected for this research due to the balance of high heat deflection temperature, dielectric strength and low viscosity. Additionally, the E1660 ink (Ercon Inc., Wareham, MA) was selected based on low average volume resistivity (2.7×10^{-7} Ω-m or 27 μΩ-cm) across a variety of substrates. However, the large particle sizes in the E1660 inks also restrict which printing technologies and nozzle sizes can be used and consequently can also limit the spatial resolution of final conductor traces. In addition to the E1660 ink, the *in situ* laser curing experiment was repeated with different inks having structure and compositions fundamentally different than the E1660 ink. As part of this investigation the CCI-300 nanoparticle ink (Cabot, Boston, MA), CB-100 conductive via plug, and CB-028 (DuPont Microcircuit Materials, Research Triangle Park, NC) were analyzed. The inks selected for this experiment had properties fundamentally different that the E1660 ink including particle structures, binder/carrier type, and particle size, as summarized in Table 4.1.

Table 4.1. Different inks utilized for laser curing experiments

Ink	Size of Silver Particles (μm)	Structure of Particles	Color of Ink Mixture	Viscosity (Pa-s)	Recommended Curing Conditions	Volume Resistivity after Curing (μΩ-cm)
Ercon E1660	20	Flake based	Silvery	18.75	138°C for 15 minutes	12.7 - 30.48
Dupont CB028	1 - 10	Flake based	Grey	15 – 30	160°C for 60 minutes	17.8 – 25.4
Dupont CB-100	1 - 5	One part silver epoxy system	Silvery	115 – 145	Drying: 110°C for 30 minutes Curing: 160°C for 60 minutes	127 – 254 (unplated)
Cabot CCI-300	0.020	Nanoparticle silver	Green	0.011 – 0.015	100 – 350°C for 1-30 minutes	4 - 80

4.3 Investigation of *In Situ* UV Laser Curing of Silver-Based Conductive Ink:

4.3.1 Introduction

Lopes et al. (2010) developed a sequence of processes to fabricate 3D dielectric structures, place components within these structures and route multilayer electrical interconnect among the components to complete the structural electronics circuits. The manufacturing process included a sub-process for intermediate *in situ* UV laser curing (at 355 nm) of the conductive ink traces. Medina et al. (2005) demonstrated the utilization of the diode-pumped solid-state (DPSS) SL laser (Series 3500-SMPS, DPSS Lasers Inc., Santa Clara, CA) to cure conductive inks sufficiently to continue SL build without contamination between the liquid ink and SL resin.

As part of this research, Lopes et al. (2010) performed a simple steady-state experiment that related incident laser beam power to the corresponding steady-state substrate temperatures. This helped determine the laser energy absorption behavior of both the SL resin and the particulate silver-based ink. A Keithley 2000 series multimeter (Keithley Instruments Inc., Cleveland, OH) was used to measure the thermistor resistance while focusing the laser on the thermistor under the following experimental conditions: (1) on the bare thermistor, (2) with two standard build layers (~203.2 μm) of cured SL resin on top of the thermistor, and (3) with an additional ~140 μm layer of uncured ink on top of the cured SL resin layer. For this experiment, the steady-state temperature measurements were 83°C for the bare thermistor, 75.5°C with the cured SL resin layer on top, and 47°C with the additional ink layer. The degree of energy absorption by SL resin and the ink explains the difference between the temperatures sensed by the thermistor. The reflectivity of silver in the UV spectrum is very complex and varies rapidly

from ~0% at laser wavelengths of 316 nm to over 90% at 375 nm with a reflectivity of ~85% at 355 nm (Hecht, 2002). As a result, the high reflectivity of silver at 355 nm may help explain the reduced energy absorption by the silver particles resulting in a lower measured thermistor temperature for this experimental condition. Early generation SL systems utilized a continuous laser at 325 nm wavelength and may present a viable alternative for improved laser curing of silver inks.

Based on these results, Lopes et al. (2010) further explored the effect of the number of laser scans on ink resistance for scanning directly on the ink trace as well as next to the ink trace on the SL substrate. This experiment examined the effect of repetitive laser scanning on final trace resistance when scanning on top of the ink trace as well as on the SL resin in the vicinity of the trace. The experiment is explained in greater detail in Lopes et al. (2010). Briefly, a sample test piece with four channels, 381 μm (0.015") wide, 406.4 μm (0.016") deep, and 11mm long, was fabricated using SL and the E1660 particulate silver-based ink was deposited in the channels. Separate laser scanning _stl' files having width of 254 μm (0.010") were created to replicate different laser scanning locations. The separate laser curing _stl' files were utilized to cure the ink traces at ~95 mW laser power with ~480 μm/s scan speed. The results indicated that laser curing profile at the scanning location ~~o~~n edge" (~190 μm [0.0075"]) from the center of the channel or centered on the edge of the substrate/ink interface with half of the beam exposing ink and the other half on the substrate) provided the lowest measured trace resistance after 12 laser scanning passes, followed by ~~o~~n ink" (centered on the ink within the channel) (Lopes et al., 2010). However, repeated scanning of the SL substrate and/or ink by the laser resulted in charring of the substrate (Figure 4.2(a)) and/or discoloration of the cured ink (Figure 4.2(b)), respectively as seen in Figure 4.2.

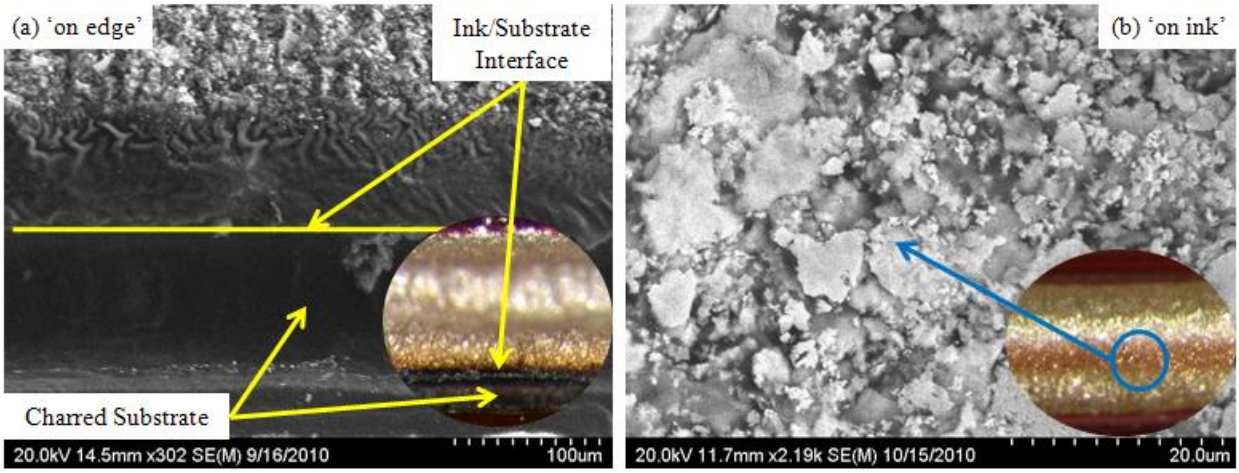

Figure 4.2. SEM images of ink/substrate; (a) 'on edge' cure, (b) 'on ink' cure; Inset: Optical microscopic images of ink/substrate

The SEM examination of the cured ink traces showed no morphological difference between the laser cured ink and a thermally cured ink. However, there is evidence of charring of the SL substrate when the laser scans directly on the substrate while providing the same laser energy. Charring of SL substrate during the SL build can lead to bonding issues between the charred SL layer and the next SL build layer. This can result in structural imperfections and in extreme may result in build failure. As a result, further investigation was necessary of the effect of laser curing using different laser parameters (laser power and scan speed) for a scanning location on the substrate adjacent to the ink channel and on the edge of the ink channel (half ink, half substrate), while providing the same laser energy, as the laser curing conditions mentioned before in an attempt to minimize resistance while avoiding charring of the SL substrate. The following sections describe the extensive *in situ* laser curing experiment that facilitated effective ink curing without undue increases in the manufacturing time.

4.3.2 Structural Effects of Repetitive Laser Scanning on Ink and Substrate

Ink curing typically involves a thermal curing process that results in solvent evaporation followed by curing of a resin binder, which facilitates the electrical interconnection between the silver particles. However, thermal curing during 3D structural electronics fabrication requires exchange of fabricated parts between the hybrid SL/DP system and a temperature oven for each embedded conductive trace routing layer. As a result, *in situ* UV laser curing of conductive inks is required for continuously fabricating structural electronic devices without intermediate exchange of a part in fabrication between the SL/DP machine and the curing oven. This is important because accurate registration is very difficult to maintain when switching between SL and DP. However, as explained in the earlier section, a significant amount of incident UV laser energy was reflected by the silver particles in the ink solution.

Based on the results of previous experiments, curing the ink trace using high laser power at slow scan speeds resulted in discoloration of the ink and/or charring of the SL substrate. As a result, it was determined to investigate the structural effects of laser curing the ink trace at relatively faster scan speeds and lower laser power, while providing the same total laser energy. The goal of this experiment was to explore the minimum number of laser passes required for effective curing of the E1660 conductive ink without charring the SL substrate. Several laser curing parameters including laser energy (laser power, scan speed) and scanning location were analyzed as part of this laser curing experiment.

Figure 4.3 illustrates the different scanning locations analyzed for this experiment: 1) _on both edges‘ in which the laser scanned half on ink and half on substrate for both sides of the ink trace, 2) the _on ink‘ in which the scanning location is entirely on the ink and centered in the

channel, and 3) ‗adjacent' in which the scanning location is on the SL substrate adjacent to both edges of the ink channel.

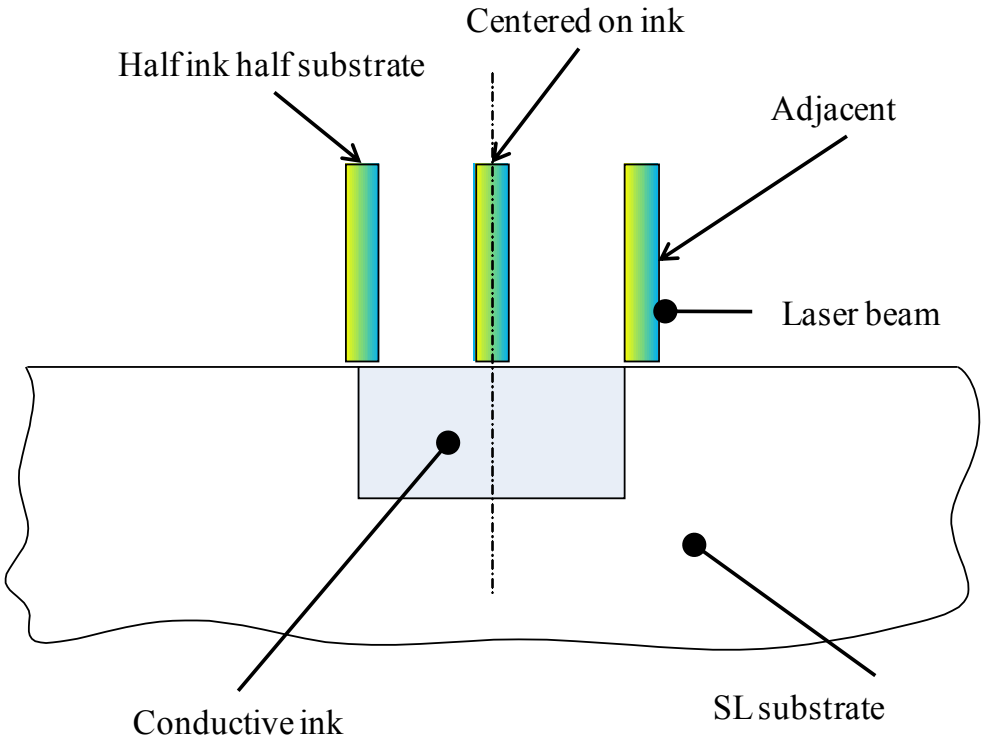

Figure 4.3. Illustration of different scanning locations analyzed during laser curing

The resulting trace resistances as well as the discoloration and charring effects, on the ink and SL resin respectively, were compared for each laser scanning condition. The change in trace resistance was recorded every ~5J of energy supplied (recorded as number of laser passes) and the number of laser passes for each laser curing condition was adjusted to ensure that the same energy (~5J) as the ‗on ink' and ‗on edge' cases was supplied. As a result, each scan was repeated as often as necessary to transmit the same total energy which included two times for the ‗adjacent faster' and ‗on both edges faster' laser curing conditions, three times for ‗adjacent faster (low power)' laser curing condition, and fourteen times for the ‗adjacent fastest' and ‗on both edges fastest' laser curing conditions. Figure 4.4 illustrates the SEM images of the ink

cured using faster speed and lower power as compared to the ‗on edge' curing condition and the experimental results from this experiment are summarized in Table 4.2 below.

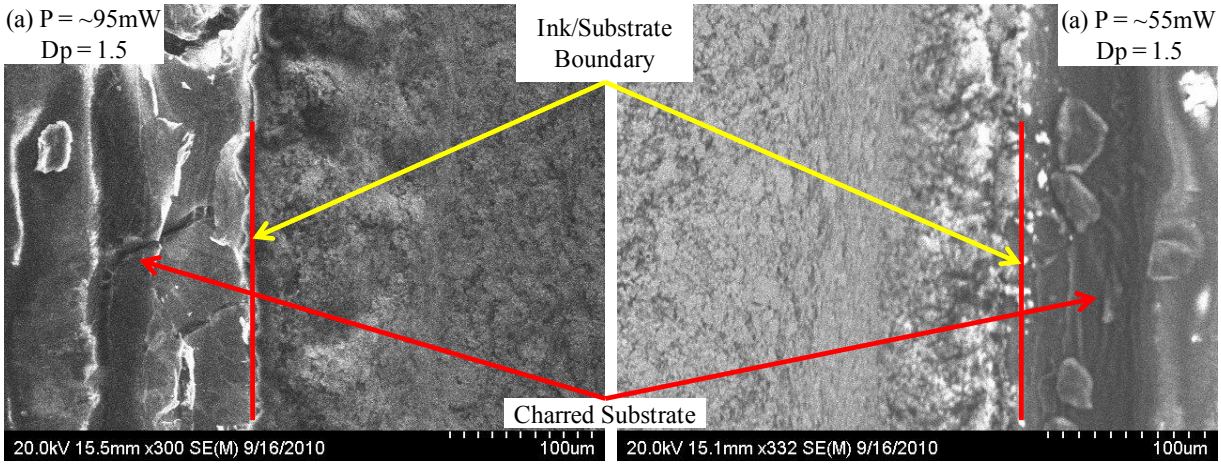

Figure 4.4. SEM images of ink cured using different laser curing conditions

Although the ‗on edge' curing case did present the best condition for laser curing the ink in terms of lowest measured trace resistance, the substrate material was severely charred by the high laser power and low traverse speed(see Figure 4.2(a)). For laser curing conditions ‗adjacent faster' and ‗adjacent low power', the substrate was also charred although they was relatively less charring (Figures 4.4 (a) and 4.4(b)) when compared to the ‗on edge' curing condition (high laser power at low scan speeds). The charring effect similar to the ‗adjacent faster' condition was seen for the ‗on both edges faster' laser curing condition. The charring of the SL substrate decreased as laser power decreased and/or scan speed increased while supplying the same laser energy. However, the resulting trace resistance values using low power and increased scan speed were also higher. Further experimentation was conducted to find the laser curing condition that did not char the SL substrate while scanning on the ‗adjacent' scanning location. It was determined that the ‗adjacent fastest' and ‗on both edges fastest' laser curing condition (~95 mW laser power and ~13500 µm/s) did not char the SL substrate while providing the same laser energy as the other laser curing conditions due to the lower instantaneous power. However, this

laser curing condition also resulted in the highest measured trace resistances as compared to the other curing conditions, as seen in Figure 4.5. Table 4.2 summarizes the results of the different experimental conditions that were compared as part of the follow-on laser curing experiment.

Table 4.2. Different laser curing parameters and terminology

	SL Parameters (Critical Exposure E_c = 11.8 mJ/Cm^2		**Laser Scanning Conditions**			**Supplied Laser Energy**			
Laser Curing Condition	**Laser Power (mW)**	**D_p**	**Scan Speed (µm/s)**	**Time/ scan (Secs)**	**No. of Scans**	**Total Energy (J)**	**% difference from nominal**	**Observation**	**Measured Trace Resistance (12 passes Avg.) (Ω)**
*_on ink‘	~95	1.25	~480	~54.25	1	~5.15	0	Discoloraton	1.77
*_on edge‘	~95	1.25	~480	~54.25	1	~5.15	0	SL Charring	1.33
_on both edges faster‘	~95	1.5	~1925	~27	2	~5.13	-0.3	SL Charring	2.3
_on both edges fastest‘	~95	2	~13500	~3.85	14	~5.1	-0.9	No SL Charring	44.30
_adjacent faster‘	~95	1.5	~1925	~27	2	~5.13	-0.3	SL Charring	1.82
_adjacent faster (low power)‘	~55	1.5	~1675	~31	3	~5.11	-0.7	SL Charring	9.125
_adjacent fastest‘	~95	2	~13500	~3.85	14	~5.1	-0.9	No SL Charring	38.87

* - Data from previous work

In summary, the results indicate that the conductive ink trace can be cured by irradiating the laser directly on the ink, the substrate, or the edge (half ink, half substrate) with respect to the ink channel. Laser curing (~95 mW laser power and ~480 µm/s scan speed) on the edge of the channel gave the lowest trace resistance, but charred the SL substrate. Alternatively, the laser conditions (~95 mW laser power and ~13500 µm/s scan speed) which did not char the SL

substrate resulted in the highest measured trace resistance. Irradiating the laser on the ink did not damage the ink, as per the SEM images, or the substrate, while providing trace resistances within 0.4 Ω of the resistance reading for _on edge' laser curing condition and - as described in the next section – are equivalent after a full oven post-cure after the fabrication process is complete.

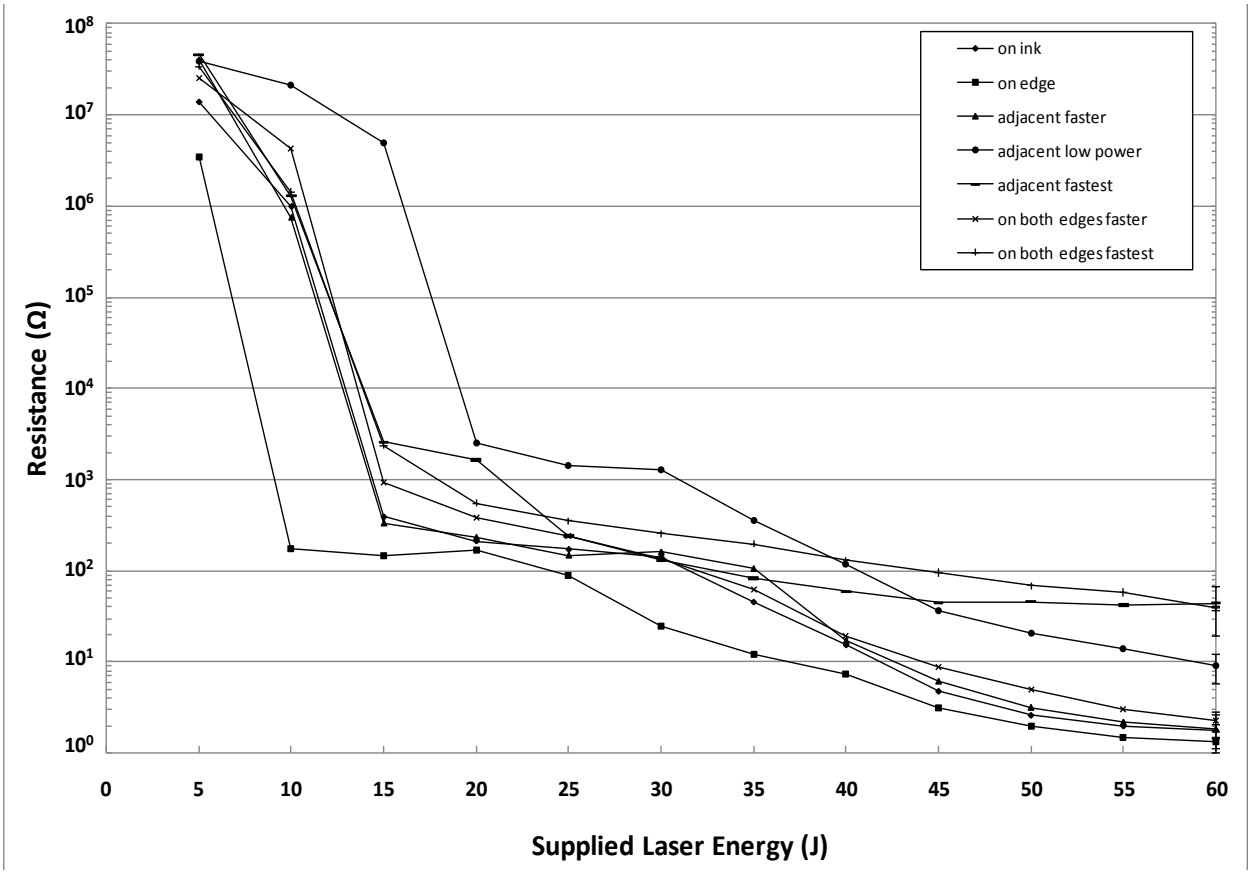

Figure 4.5. Effect of different laser curing conditions on trace resistance

(Error bars shown at 60 J represent ± 1 standard deviation; Error bars not shown at other data points for clarity; n=4)

4.3.3 Effect of Additional Oven Curing on Trace Resistance

Due to the various options available to laser cure a conductive ink, it was worthwhile to investigate the impact of thermal post-cure process on partially laser cured conductive ink traces embedded in SL resin. The purpose of this experiment was to investigate the feasibility of

eliminating the need for full laser cure of embedded DP traces by determining the minimum number of *in situ* laser scanning passes required during fabrication. In general, oven curing is preferred as the SL tool is made available for additional high value production, and oven curing processes the entire system including multiple layers of conductive traces simultaneously. However, oven curing required the printed traces to be cured while being completely embedded in an SL structure, whereas the laser curing was completed with the ink exposed to the ambient – potentially improving the process as binder and solvent are more readily released. Given the potential beneficial aspects of a follow-on cure in terms of reducing overall processing time, several laser curing parameters including laser power, scanning locations, scan speeds, and number of laser passes, were examined in the context of a follow-on oven cure to identify the best pre-cure laser process . These laser scanning parameters are summarized in Table 4.3.

Table 4.3. Laser curing samples for examining oven curing effects on trace resistance

Laser Scanning Location	Laser Power (mW)	Scan Speed (μm/s)	Scanning Time (s)	Energy Supplied (J)
'on ink'	~95	~480	54, 270, 648	5, 25, 60
'on edge'	~95	~480	648	60
'on SL adjacent'	~95	~1925	54, 270, 648	5, 25, 60
	~55mW	~1675	648	60

The E1660 conductive ink was dispensed in the ink trace and cured as per each given laser parameter in Table 4.3. The DP traces on these samples were embedded using the ProtoThermTM 12120 resin, which was dispensed using a syringe and cured using an UV light source (Green Spot, UV Source, American Ultraviolet Company, Torrance, CA). A Fluke 287 True RMS Multimeter (Fluke Corp., Everett, WA) was utilized to measure the trace resistances on all samples before and after oven curing the samples at 80oC for 16 hours. Although not a

complete statistical study, the preliminary results, as shown in Figure 4.6, indicate that oven curing enhances the conductivity (or lowers the measured resistance) of an ink trace regardless of its initial laser cured state. Additionally, the final post oven-cured resistance depended on the initial trace resistance.

As seen from the Figure 4.6, increasing the laser scanning passes prior to embedding the conductive traces resulted in a lower measured trace resistance after oven curing. An interesting observation was that the _on ink' laser condition after 60 J and the _on edge' condition after 60 J had the same trace resistance (0.3Ω), after additional oven cure although the –on edge" was lower prior to the oven cure. However, the resistance reduction may be limited by embedding partially cured ink traces within an SL resin channel as all embedded trace resistances after oven curing were greater than the calculated ideal cured trace resistance for the ink channel (~0.2 Ω, including probe resistance of 0.15 Ω; assuming 50% shrinkage), based on the following equation. Consequently, the complexity and power requirements of the electrical circuits will determine the minimum trace resistance required for ensuring functionality.

Where R = Ink trace resistance

ρ = Volume resistivity as per data sheet (12.7 - 30.48 μΩ-cm)

L = Distance between multi-meter probes (1.3 cm)

W = width of the ink trace (~380 μm)

T = thickness of the ink trace (~200 μm based on ~50% shrinkage due to curing)

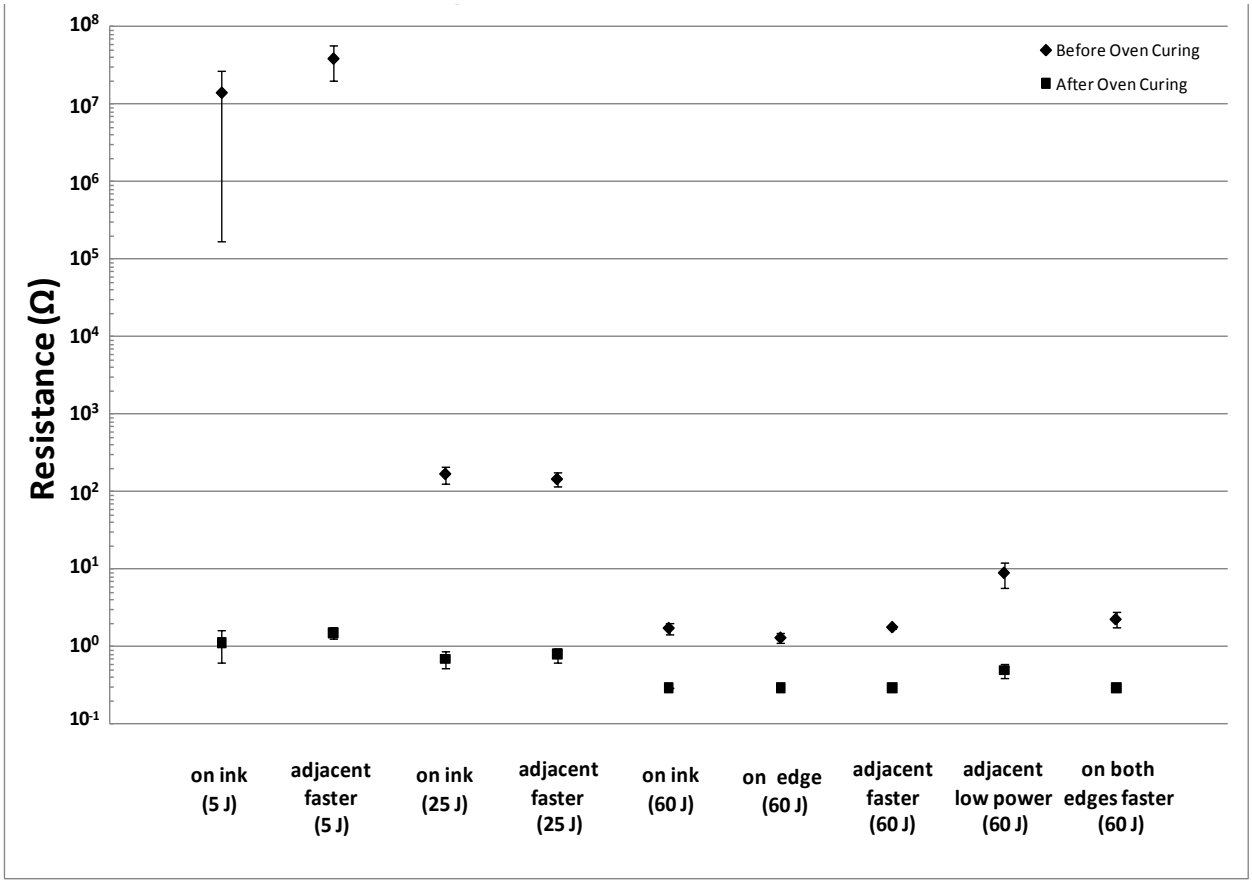

Figure 4.6. Effect of oven curing on trace resistance of different laser cured ink traces (Error bars represent ± 1 standard deviation; Error bars not seen in the graph are within the markers; Errors bar show non-uniform standard deviation due to the Log scale; n=3)

Based on the results, a combined procedure involving partial laser curing of conductive traces to eliminate contamination between SL resin and uncured ink during fabrication and post fabrication thermal curing to minimize trace resistance was determined to be the optimal ink curing procedure for 3D Structural Electronic fabrication.

4.3.4 Effect of Laser Curing on Different Inks

Based on the observations from previous results, there was a need to investigate the effect of laser curing procedure on a wide variety of conductive inks – including those that are fundamentally different structurally from the E1660 conductive ink used for this research. As a result, the following experiments were performed to examine whether the above laser curing results can be generalized. For this experiment, the ‗on ink' laser curing condition (‗on ink' scanning location, ~95 mW laser power, ~480 μm/s scan speed) was repeated for different types of ink. As part of this investigation the CCI-300 nanoparticle ink, CB-100 conductive via plug, and CB-028 were analyzed. The inks selected for this experiment had properties fundamentally different than the E1660 ink as described in section 2.2.

As shown in Figure 4.7, the ‗on ink' laser curing condition which effectively cured the E1660 ink was ineffective for inks with fundamentally different particle structure, binder base, and viscosity. Laser curing of the CB 100 conductive via plug did not record any reading on the multi-meter and hence was not included in the graph. The relatively higher temperature curing conditions and high viscosity, as stated in the graph, coupled with high reflectivity of silver at 355nm wavelength can help to explain the lack of conductivity for the CB100 ink. This indicates that the laser energy did not heat the ink sufficiently to initiate any curing in the ink trace. Similarly, the CCI-300 nanoparticle silver ink demonstrated ineffective curing using the given laser curing condition. For nanoparticle silver based inks conduction occurs by sintering of individual nanoparticles via thermal curing of the ink mixture at a high temperature (>100°C). As a result, nanoparticle inks and high temperature curing inks require a much higher laser power to induce effective laser ink curing (>100 mW; (Bieri et al., 2003; Chung et al., 2004; Fearon et al., 2007; Maekawa et al., 2009): Note that the 355nm laser can be safely used up to

100 mW). The CB028 ink was structurally most similar to the E1660 ink but demonstrated trace resistances that were comparatively higher when compared to the E1660 ink. The observed differences between these two inks were the color of the ink mixture (E1660 was silvery and CB028 was greyish) and the size of the flakes. Consequently, the color of the solvent and binder base seems to have affected affect the absorption of laser energy by the conductive particles and subsequently the ink curing effectiveness (Hecht, 2002). Also the smaller silver flakes coupled with relatively poor solvent evaporations might have reduced the percolation effect in the CB028, which led to the higher trace resistances. In summary, the 355nm wavelength laser cannot be utilized for curing all commercially available conductive inks. It appears that high viscosity and high curing temperatures are undesirable properties while considering conductive inks for UV laser curing at lower laser powers (<100mW). Furthermore, each ink solution needs to be structurally analyzed (particle shape and color of mixture) in order to determine the most effective laser curing parameters, including laser wavelength for satisfactory conductive ink curing. Although not a statistical study, this experiment helps understand the important parameters that need to be considered for selecting conductive inks for laser curing. Future work is needed to analyze the different solvent bases to determine the laser parameters (energy and wavelength) needed for effectively curing a variety of inks and help generalize the laser curing process.

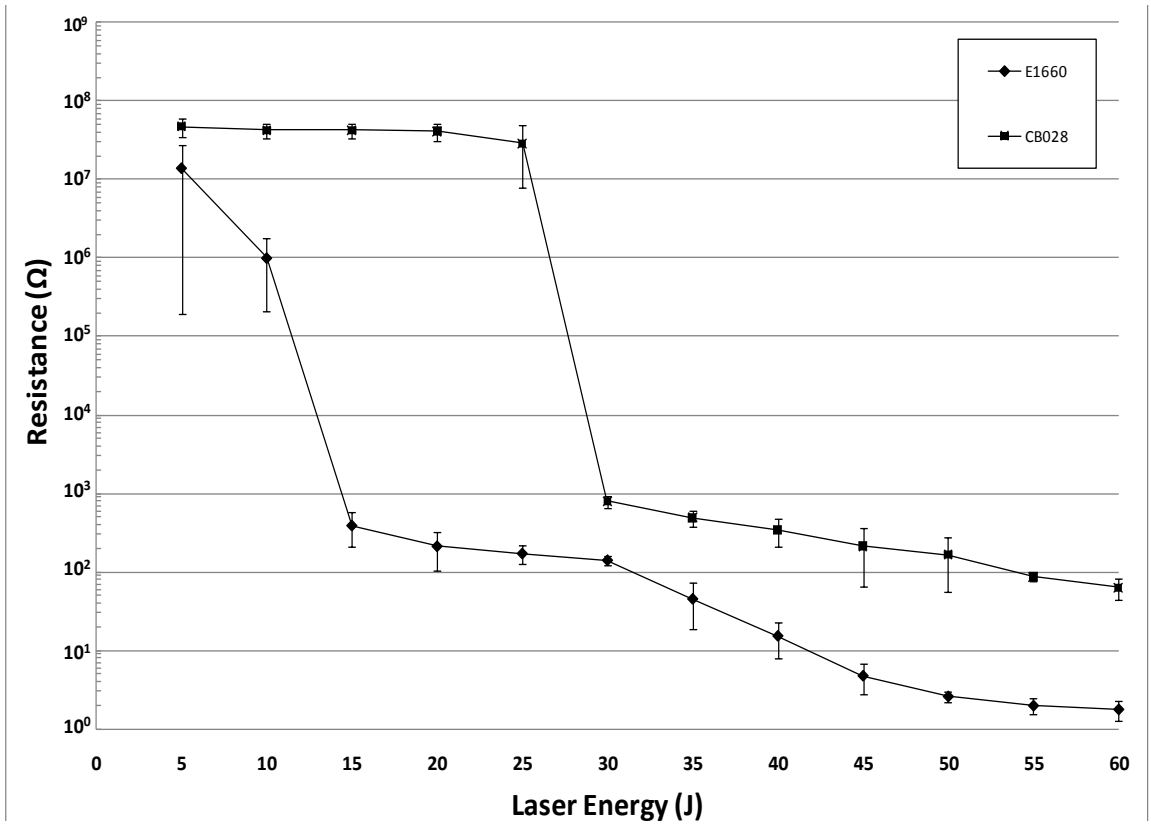

Figure 4.7. Laser curing effect on trace resistance for different inks; X-axis shows the energy supplied after each laser pass which took ~54 seconds at ~95 mW laser power (Error bars represent ± 1 standard deviation; Errors bar show non-uniform standard deviation due to the Log scale; n=4)

4.3.5 Effect of Laser Wavelength on Trace Resistance

The results from previous experiments helped determine the most effective scanning location and conductive ink using the 355 nm SL laser. However, due to the high reflectivity of silver at 355 nm, it was determined to investigate the effectiveness of ink curing, measured in terms of trace resistance, at a wavelength close to 316 nm (100% absorption, Hecht, 2002). Earlier versions of SL systems utilized a 325 nm HeCd laser, but the short product life resulted in the shift towards the 355 nm wavelength DPSS laser for SL fabrication. Despite this limitation, the reflectivity graph of silver provided an opportunity to analyze the 325 nm wavelength laser as a source for curing conductive inks. As a result, this experiment was carried out using a 325

nm wavelength HeCd laser (Omnichrome, Series 74) keeping all other laser curing conditions similar to the 355nm DPSS laser. Specifically, the _on ink' laser curing condition (_on ink' scanning location, ~95 mW laser power, ~480 µm/s scan speed) carried out at 355 nm in the earlier section, was repeated using a 325 nm wavelength. The E1660 silver-based conductive ink was deposited in a channel 381 µm (0.015") wide, 406.4 µm (0.016") deep, and 11mm long. A separate laser scanning _stl' file having width of ~250 µm (0.010") was created to replicate the _on ink' scanning location. The _stl' file was utilized to cure the ink traces at 17 mW laser power for ~300 secs to provide the same energy per data point (~5J) as the _on ink' experiment with the 355nm DPSS laser at ~95 mW for ~54 secs. The resistance across the trace was recorded three minutes after every 5J of energy supplied using a Keithley 2000 series multimeter. The results are summarized in Figure 4.8. For the E1660 ink, the results indicate that laser curing at 325 nm wavelength seems to be more effective in curing the conductive trace as compared to the 355 nm wavelength during the first phase of ink curing process (up to 30 J of energy supplied). Hecht, (2002) have illustrated that silver exhibits maximum absorption at a wavelength ~316 nm. However the effectiveness of the subsequent laser energy supplied reduced and the trace resistances converged within 0.5Ω after 12 passes for the two wavelengths. There was also no evidence of discoloration on the ink trace (as seen in section 3.2 while using the 355 nm laser) when laser curing at 325 nm wavelength due to a more uniform energy distribution as a result of the relatively higher laser energy absorption by the silver particles (see Figure 4.8: Inset, Hecht, 2002).

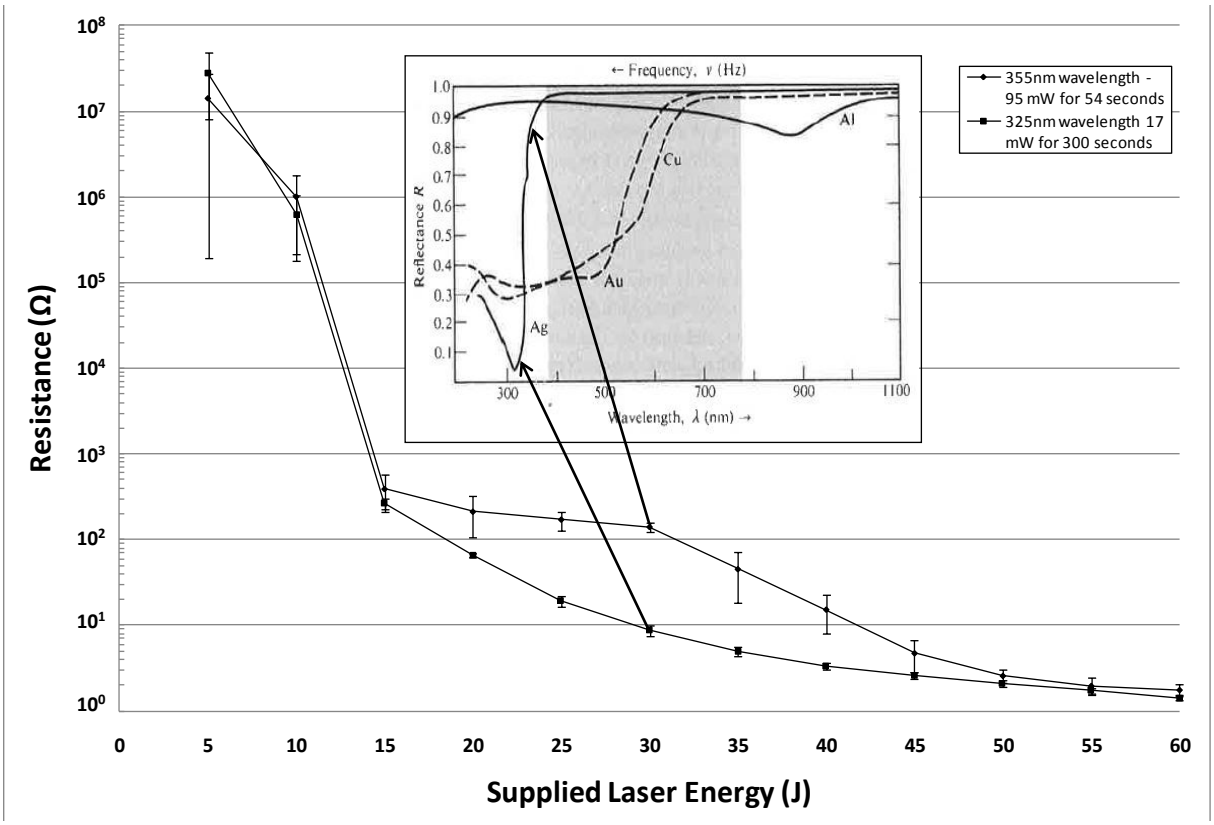

Figure 4.8. Effect of laser wavelength on trace resistance for on-ink laser curing; (Error bars represent ± 1 standard deviation; Error bars not seen in the graph are within the markers; Error bars show non-uniform standard deviations due to the Log scale; n=4) Inset: Reflectance vs. wavelength curves for Au, Ag, Al, and Cu, Hecht, 2002)

The genesis X-ray microanalysis software (EDAX®, Mahwah, NJ) was utilized to perform qualitative materials analysis on the cured ink analysis on the ink traces cured using the laser beam at 325 nm and 355 nm wavelengths and the results are illustrated in Figure 4.9. As seen in the figure, laser curing at 355 nm (Figure 4.9(a)) displays identical peaks as compared to laser curing at 325 nm wavelength (Figure 4.9(b)). Although the base elements within the laser cured inks using the 325 nm and the 355 nm wavelengths were the same, the slightly different counts at ~0.5 keV may suggest that the high energy 355 nm wavelength laser conditions resulted in oxidation of the cured ink due to excessive heating (recall the discoloration). The

results indicate that the 325 nm wavelength seems to perform better than the 355 nm wavelength for curing silver particulate based conductive inks using a UV laser while supplying the same laser energy. However, further experiments at the same laser power and scans speeds for both the 355 nm and 325 nm wavelengths are required to confirm these conclusions.

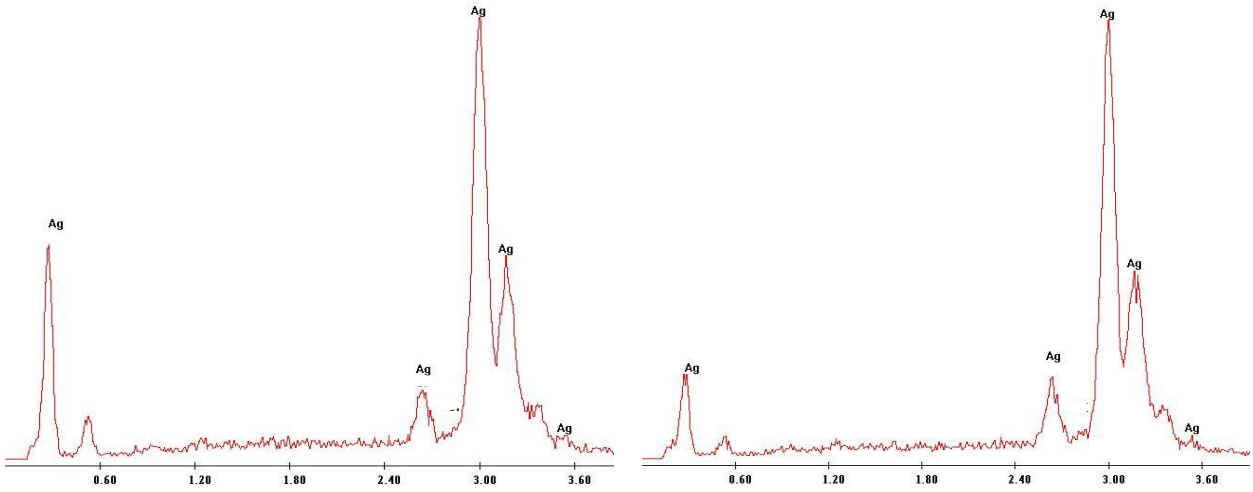

(a) (b)

Figure 4.9. Qualitative materials analysis of laser cured inks using EDAX® genesis x-ray microanalysis software: (a) at 355nm, (b) at 325 nm

4.4 Conclusions:

This paper presents the results of various UV laser curing experiments to determine the conditions for most effective laser curing of conductive ink traces *in situ* within a stereolithography system. As a result, an *in situ* UV laser curing process was developed to sufficiently cure the conductive ink traces to enable fabrication of 3D electronic circuits without removal of the part from the SL/DP machine during fabrication. The experimental results indicate that a standard SL DPSS laser with 355 nm wavelength can be utilized to cure the conductive trace effectively at a temperature of 80°C without damaging the reflecting mirrors in the SL machine. Thus the laser curing process described in this research can be utilized in any commercially available SL system. Moreover, two strategies for successful *in situ* UV laser ink curing, without charring the substrate while providing the same laser energy, can be proposed; (1) direct irradiation onto the ink with higher instantaneous laser energy, and (2) irradiation of laser onto the substrate with lower instantaneous laser energy, several times. Direct irradiation on the ink using the 355 nm wavelength laser resulted in trace resistances comparable to the ‗on edge' curing condition. However there was evidence of discoloration of the cured ink as seen from the optical microscope although SEM analysis revealed no structural damage.

Laser curing (~95 mW laser power and ~480 μm/s scan speed) on the edge of the channel gave the lowest trace resistance, but charred the SL substrate. Additionally, the oven curing experiments indicated that the post oven-cured trace resistances were similar given the same partial laser cured condition. Irradiating the substrate with lower instantaneous laser energy took longer due to necessary additional repetitions of laser scanning and also resulted in the least effective curing in terms of resistivity.

Additionally, preliminary experiments determined that thermal post-curing of partially cured ink traces enhances the conductivity of an embedded trace regardless of initial cured state, thereby eliminating the need for complete laser curing prior to embedding the trace. As a result, a combination of post-fabrication thermal curing process and a partial laser pre-cure of embedded ink traces was proposed, to decrease overall fabrication time. The embedded ink traces can be partially laser cured to avoid contamination between the SL resin and semi-solid conductive ink and fully cured during the final oven curing process. It should be noted that the complexity and power requirements of the electrical circuits will determine the minimum trace resistances required for ensuring functionality. Laser curing at 325 nm wavelength demonstrated better volumetric ink curing as compared to the 355 nm wavelengths for curing silver particulate based conductive inks due to the higher energy absorption. The laser curing condition which effectively cured the E1660 ink were found to be ineffective for inks with different size silver particles, colored solvents, resin binder base, high curing temperatures and high viscosity. Such inks require laser sources with considerably higher power capabilities. As a result, *in situ* UV laser curing using the SL laser is limited for conductive inks that require low temperature (laser power < 100 mW) for effective curing. Further research should focus on understanding the effects of different laser power, wavelength, and scan speed to help determine the limitations of the laser conductive trace curing process and its effect on the functionality of the 3D structural electronic devices.

4.5 References:

Banfield, D., 2000. Understanding and measuring electrical resistivity in conductive inks and adhesives. SGIA Journal.

Bieri, N., Chung, J., Haferl, E., Poulikakos, D. and Grigoropoulos, C., 2003. Microstructuring by printing and laser curing of nanoparticle solutions. Applied Physics Letters 82 (20), 3259-3531.

Chrisey, D.B. and Piqué, A., 2002. Direct-Write Technologies for Rapid Prototyping Applications: Sensors, Electronics, and Integrated Power Sources. Harcourt Inc.: Academic Press, San Diego, California.

Chung, J., Bieri, N.R., Ko, S., Grigoropoulos, C. and Poulikakos, D., 2004. In-tandem deposition and sintering of printed gold nanoparticle inks induced by continuous Gaussian laser irradiation. Applied Physics A 79, 1259-1261.

Church, K.H., Fore, C. and Feeley, T., 2000. Commercial applications and review for direct write technologies. Materials Development for Direct Write Technologies 624, 3-8, San Francisco, CA, April 24-26.

Fearon, E., Sato, T., Wellburn, D., Watkins, K. and Dearden, G., 2007. Thermal effects of substrate materials used in the laser curing of particulate silver inks. Laser Assisted Net Shaping Engineering 5-Proceedings of the LANE. 379-390.

Greer, J.R. and Street, R.A., 2007. Thermal cure effects on electrical performance of nanoparticle silver inks. Acta Materialia 55, 6345–6349.

Hecht, E., 2002. Optics, 4th Edition, Published by Addison and Wesley, San Francisco, CA, ISBN 0-8053-8566-5.

Jacobs, P.F., 1992. Rapid prototyping & Manufacturing: Fundamentals of stereolithography, Published by Society of Manufacturing Engineers, Dearborn, Michigan.

Jagt, J., 1998. Reliability of electrically conductive adhesive joints for surface mount applications: a summary of the state of the art. IEEE Transactions on Components, Packaging, and Manufacturing Technology—Part A 21(2), 215-225.

Kim, D. and Moon, J., 2005. Highly conductive inkjet printed films of nanosilver particles for printable electronics. Electrochemical and Solid State Lasers 8(11), 130-133.

Ko, S.H., Choi, Y., Hwang, D., Grigoropoulos, C., Chung, J. and Poulikakos, D., 2006. Nanosecond laser ablation of gold nanoparticle films. Applied Physics Letters 89, 141126-1-3.

Lopes, A.J., Navarrete, M., Medina, F., Palmer, J., MacDonald, E. and Wicker, R.B., 2006. Expanding rapid prototyping for electronic systems integration of arbitrary form. Proceedings of the 17th Annual Solid Freeform Fabrication Symposium, University of Texas at Austin, Austin, TX.

Lopes, A.J., MacDonald, E. and Wicker, R., 2010. Integrating stereolithography and direct print technologies for 3D structural electronics fabrication Rapid Prototyping Journal. To Appear.

Maekawa, K., Yamasaki, K., Niizeki, T., Mita, M., Matsuba, Y., Terada, N. and Saito, H., 2009. Influence of wavelength on laser sintering characteristics of Ag nanoparticles. Electronic Components and Technology Conference, 1579 – 1584.

Malone, E. and Lipson, H., 2006. Freeform fabrication of ionomeric polymer-metal composite actuator. Rapid Prototyping Journal 12(5), 244-253.

Medina, F., Lopes, A.J., Inamdar, A., Hennessey, R., Palmer, J., Chavez, B., Davis, D., Gallegos, P. and Wicker, R.B., 2005. Hybrid manufacturing: integrating stereolithography and direct write technologies. Proceedings of the 16th Annual Solid Freeform Fabrication Symposium, University of Texas at Austin, Austin, TX, 39-49.

Mo, L., Liu, D., Zhou, X. and Li, L., 2009. Preparation and conductive mechanism of the ink-jet printed nanosilver films for flexible display. 2nd International Congress on Image and Signal Processing, ISBN # 978-1-4244-4129-7.

Palmer, J.A., Yang, P., Davis, D.W., Chavez, B.D., Gallegos, P.L., Wicker, R.B. and Medina, F.R., ,2004. Rapid prototyping of high density circuitry. Rapid Prototyping & Manufacturing 2004 Conference Proceedings, Rapid Prototyping Association of the Society of Manufacturing Engineers, Hyatt Regency Dearborn, Michigan. Also, SME Technical Paper TP04PUB221 (Dearborn, Michigan: Society of Manufacturing Engineers).

Palmer, J.A., Summers, J.L., Davis, D.W., Gallegos, P.L., Chavez, B.D., Yang, P., Medina, F. and Wicker, R.B., 2005. Realizing 3-D interconnected direct write electronics within smart stereolithography structures. International Mechanical Engineering Congress and Exposition 2005 Proceedings, November 14-18, Orlando, Florida.

Park, B. K., Kim, D., Jeong, S., Moon J. and Kim, J. S., 2007. Direct writing of copper conductive patterns by ink-jet printing. Thin Solid Films 515, 7706–7711.

Periard, D., Malone, E. and Lipson, H., 2007. Printing embedded circuits. Proceedings of the 18th Solid Freeform Fabrication Symposium, Austin TX, 503-512.

Piqué, A., Mathews, S.A., Pratap, B., Auyeung, R.C.Y., Karns, B.J. and Lakeou, S., 2006. Embedding electronic circuits by laser direct-write. Microelectronic Engineering 83, 2527-2533.

Pudas, M., Halonen, N., Granat, P. and Vahakangas, J., 2005. Gravure printing of conductive particulate polymer inks on flexible substrates. Progress in Organic Coatings54,310–316.

Robinson C.J., Stucker B., Lopes A.J., Wicker R.B. and Palmer J.A., 2006. Integration of direct-write (DW) and ultrasonic consolidation (UC) technologies to create advanced structures with embedded electrical circuitry. Proceedings of the 17th Annual Solid Freeform Fabrication Symposium, University of Texas at Austin, Austin, TX, pp. 60-69.

Saraf R.F., Roldan J.M., Jagannathan R., Sambucetti C., Marino J., Jahnes C., 1995. Polymer/metal composite for interconnection technology. Proceedings of the 45th Electronic Components and Technology Conference, pp. 1051–1053.

Young, D., Sampath, S., Chikov, B. and Chrisey, D.B., 2005. The future of direct writing in electronics. CircuiTree.

Weiss, L.E., Merz, R., Prinz, F.B., Neplotnik, G., Padmanabhan, P., Schultz, L. and Ramaswami, K., 1997. Shape deposition manufacturing of heterogeneous structures. SME Journal of Manufacturing Systems16(4), 239-248.

Weiss, L. and Prinz, F., 1998. Novel applications and implementations of shape deposition manufacturing. Naval Research Reviews, Office of Naval Research, Three, Vol. L

DSM Somos ProtoTherm™ 12120 –Product Data Sheet, New Castle: Delaware, www.dsmsomos.com, 03/27/2005.

E1660 Product Data Sheet, www.erconinc.com, (accessed on 15 May 2010).

nScrypt Inc., http://www.nscryptinc.com/smartpump/ , (accessed 9 June 2010).

Thermometrics Inc., http://www.gesensing.com/products/resources/whitepapers/ntcnotes.pdf (accessed on 10 May 2010).

Chapter 5

5 CONCLUSIONS

This dissertation work broadly demonstrated what could be achieved by integrating multiple additive manufacturing (AM) technologies together for fabricating unique devices and more specifically demonstrated a hybrid SL/DP machine that can fabricate unique, monolithic three dimensional (3D) embedded electronic circuits. As a result, a hybrid manufacturing system that integrates stereolithography (SL) and direct print (DP) technologies to fabricate 3D structures with embedded electronic circuits was presented. A functional SL/DP manufacturing process was developed to fabricate 3D monolithic structures with embedded electronics and interconnects. The process involved part design, process planning, integrated manufacturing including multiple starts and stops of both SL and DP, *in situ* UV laser curing of conductive inks, and post-processing. The integrated 3D micro-dispensing system provided improved control over DP dispensing and combined with the manufacturing flexibility of the SL machine enabled the fabrication of a 3D electronic device within the hybrid SL/DP machine. Although the 3D structural electronic devices fabrication process does not require removal of the structure from the machine during fabrication, many of the current sub-processes are manual. As a result, further development is required for complete automation of the manufacturing process. Fabrication of simple 2D (single layer routing) and 3D (multiple layers of routing) 555 timer circuits were demonstrated using a semi-automated approach to SL/DP integration.

To enable fabrication of 3D electronic circuits without removal of the part from the SL/DP machine during fabrication, an *in situ* laser scanning procedure using the SL laser was developed that sufficiently cured the conductive ink traces in the machine so that the SL build could continue. Various laser curing experiments were carried out to determine the most effective *in*

situ UV laser ink curing condition to facilitate fabrication of 3D structural electronic devices within the hybrid SL/DP machine without removal of the part during fabrication. The experimental results indicated that the SL laser can be utilized to cure the conductive trace effectively at a temperature of 80°C without damaging the SL mirrors. The results further indicated that the conductive ink trace can be cured by irradiating the laser directly on the ink, the substrate, or the edge (half ink, half substrate) with respect to the ink channel. Laser curing (~95 mW laser power and ~480 μm/s scan speed) on the edge of the channel gave the lowest trace resistance, but charred the SL substrate. Alternatively, the laser conditions (~95 mW laser power and ~13500 μm/s scan speed) which did not char the SL substrate resulted in the highest measured trace resistance. Direct irradiation on the ink resulted in discoloration of the cured ink, as seen in an optical microscope, although no structural damage was indicated by the SEM images. The results from the UV laser curing experiments indicate two strategies for the UV laser ink curing without damaging the substrate, while providing same laser energy; (1) direct irradiation onto the ink with higher instantaneous laser energy, and (2) irradiation of laser onto the substrate with lower instantaneous laser energy, several times. To decrease fabrication time, oven curing process of partially laser cured ink traces was proposed. The results indicate that oven curing enhances the conductivity of an embedded trace regardless of initial cured state, thereby eliminating the need for complete laser curing prior to embedding the trace. Based on the results, a combined procedure involving partial laser curing of conductive traces to eliminate contamination between SL resin and ink during fabrication and post fabrication thermal curing to minimize trace resistance was determined to be the optimal ink curing procedure for 3D Structural Electronic fabrication.

Laser curing at the 325 nm wavelength demonstrated better volumetric ink curing as compared to the 355 nm wavelength for curing silver particulate based conductive inks due to the higher energy absorption. The laser curing condition which effectively cured the E1660 ink were found to be ineffective for inks with different size silver particles, colored solvents, resin binder base, high curing temperatures and high viscosity. Such inks require laser sources with considerable high power capabilities. As a result, *in situ* UV laser curing using the DPSS SL laser is limited for conductive inks that require low temperature (laser power < 100 mW) for effective curing. These experiments were limited in their scope and further research is required to understand the effects of all applicable parameters to generalize the ink curing process. This will help determine the limitations of the laser conductive trace curing process and its effect on the functionality of the electronic devices.

Opportunities exist to fully automate the hybrid SL/DP machine and fabrication process for enhancing the commercial appeal for fabricating complex systems. Laser scanning of surface contours and 3D linear positioning systems are techniques that can enable automation of the SL/DP registration and help optimize the fabrication process. Improved vertical via design, automated cleaning, and optimized laser curing can help achieve improved multilayer trace conductivity and complexity. Utilizing low shrinkage, low temperature curing ink for vertical vias can provide relatively better connections as compared to the current process. Achieving complete automation of the SL/DP process and optimizing the vertical interconnects are important areas of future research that can enable critical advancement in this technology. Incorporating surface mount components can further assist in the miniaturization of the final circuit. The 3D circuits fabricated using the hybrid SL/DP system can be tested using standard temperature, humidity, and pressure tests to determine the optimum as well as extreme operating

conditions. These tests provide valuable information about how a device will behave under extreme operating conditions, such as high/low pressure, high/low temperature, temperature shock (indicates how well a device will perform under cyclic temperature loading), and high humidity.

APPENDIX A: PERMISSION TO INCLUDE MATERIAL FROM RAPID PROTOTYPING JOURNAL

Lopes, Amit J

From: Thomas Dark [TDARK@emeraldinsight.com]
Sent: Thursday, November 25, 2010 3:05 AM
To: Lopes, Amit J
Subject: RE: Rapid Prototyping Journal - Decision on Manuscript ID RPJ-07-2010-0065.R1

Dear Amit,

Thank you for checking your dissertation chapter with me.
I can confirm that the chapter is fine to publish as it is concerning any copyright issues.
The only thing you need to bear in mind is that if it were ever to be published commercially, you would have to get in touch with us beforehand to obtain permission.

I can also confirm that I have received the updated figure 3 with the correct caption and I will upload this to go with the paper.
I wish you well in the final submission of your dissertation.

Regards,

Tom

From: Lopes, Amit J [mailto:ajlopes@utep.edu]
Sent: 23 November 2010 23:51
To: Thomas Dark
Subject: RE: Rapid Prototyping Journal - Decision on Manuscript ID RPJ-07-2010-0065.R1

Dear Tom,
Just an update on the matter of including the material in my dissertation. Our University allows me to attached an exact copy of my entire published journal paper as part of dissertation document as a separate chapter as long as we acknowledge at the beginning of the chapter that "This material is taken from the paper 'Integrating Stereolithography and Direct Print Technologies for 3D Structural Electronics Fabrication', to be published in *Rapid Prototyping Journal*, by Emerald Group Publishing".
They (Our Graduate School) already approved your email as confirmation of this. However, I want to make sure that this if OK with RPJ and Emerald.
I am attaching a PDF version of how the chapter 3 will look in my dissertation. I am hoping that I can use this copy as part of my dissertation without any further changes to the content.
Please let me know if I, as the lead author, am OK as far as copyright issues go, to include the chapter as part of my dissertation.
Thanks,
Amit

APPENDIX B: PERMISSION TO INCLUDE MATERIAL FROM JOURNAL OF MATERIALS PROCESSING TECHNOLOGY

Lopes, Amit J

From: Mahfoudh, Samir (ELS-OXF) [S.Mahfoudh@elsevier.com]
Sent: Friday, November 19, 2010 2:48 AM
To: Lopes, Amit J
Subject: STJ: Future Inquiry

Dear Amit,

Thank you for your e-mail.

Please accept this as confirmation that, as part of your author rights, you have the right to include the journal article, in full or in part, in a thesis or dissertation.

For more information on the rights you retain as a journal author, please see
http://www.elsevier.com/wps/find/authorsview.authors/copyright#whatrights

Kind regards,

Sam

Sam Mahfoudh :: Rights Assistant :: Elsevier
T: +44 (0)1865 843715 :: F: +44 (0)1865 853333
E: **s.mahfoudh@elsevier.com**

From: Lopes, Amit J [mailto:ajlopes@utep.edu]
Sent: 18 November 2010 16:57
To: Rights and Permissions (ELS)
Subject: Future Inquiry

Dear Editor,
My name is Amit Lopes and I am a Ph.D. candidate graduating this fall. I am in the process of submitting a paper to the JMPT on laser curing of silver particles. Our university allows us to use published journal papers as part of our final dissertation document. For facilitating this, I wanted to inquire if the JMPT grants permission (I read the permission form and it does have all the options I need) to include my paper in my dissertation.
Please let me know if you need more information.
Best Regards,
Amit

CURRICULUM VITAE

Amit Joe Lopes was born in Bassien, Mumbai, India and is the eldest son of Mary and Joseph Lopes. He enrolled at the Fr. Conceicao Rodrigues College of Engineering affiliated to the University of Mumbai, India in August of 1997, where he obtained a Bachelor of Engineering in Production Engineering in August of 2001. He worked as a Facilities Planning Engineering intern from November 2000 to April 2001 at Godrej and Boyce Manufacturing Limited, Mumbai, India. He decided to pursue higher education in the USA and graduated with a Master of Science in Industrial Engineering degree from the University of Texas at El Paso in July of 2003 under the guidance of Dr. Arunkumar Pennathur. He remained at the University of Texas in El Paso and pursued his Doctoral degree in the Materials Science and Engineering interdisciplinary program under the guidance of Dr. Ryan Wicker. During his graduate studies he worked as a graduate teaching and research assistant in the Materials Science and Engineering Department. As a graduate student he has been supported by a variety of scholarships and fellowships including UTEP Track and Field scholarship and the Dodson Dissertation Fellowship. He worked as an intern with Dell Inc. in 2007 and 2008 as a Process Engineer. His research work has been presented in the Solid Freeform Fabrication Symposium and accepted for publication in the Rapid Prototyping Journal.

Permanent Address:

_Regalo De Dios', 4-23 Manickpur, Vasai Rd. (W), Thane, Maharashtra P.O. 401202, India

'I firmly believe that any man's finest achievement, the greatest fulfillment of all that he holds dear, is that moment when he has worked his heart out in a good cause and lies exhausted in the field of battle—Victorious'. -- ***Vince Lombardi, Hall of Fame NFL coach, Green Bay Packers***